

ELASTIC WAVE PROPAGATION THROUGH MULTILAYERED MEDIA

D. E. Chimenti
R. L. Crane
Nondestructive Evaluation Branch
Metals and Ceramics Division

April 1980

TECHNICAL REPORT AFML-TR-79-4214

Final Report for Period May 1979 - October 1979

Approved for public release; distribution unlimited.

AIR FORCE MATERIALS LABORATORY
AIR FORCE WRIGHT AERONAUTICAL LABORATORIES
AIR FORCE SYSTEMS COMMAND
WRIGHT-PATTERSON AIR FORCE BASE, OHIO 45433

NOTICE

When Government drawings, specifications, or other data are used for any purpose other than in connection with a definitely related Government procurement operation, the United States Government thereby incurs no responsibility nor any obligation whatsoever; and the fact that the government may have formulated, furnished, or in any way supplied the said drawings, specifications, or other data, is not to be regarded by implication or otherwise as in any manner licensing the holder or any other person or corporation, or conveying any rights or permission to manufacture, use, or sell any patented invention that may in any way be related thereto.

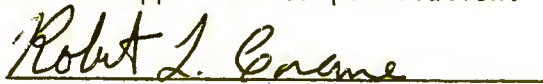
The views and conclusions contained in this document are those of the authors and should not be interpreted as representing the official policies, either expressed or implied, of the Defense Advanced Research Projects Agency or the U.S. Government.

This report has been reviewed by the Information Office (OI) and is releasable to the National Technical Information Service (NTIS). At NTIS, it will be available to the general public, including foreign nations.

This technical report has been reviewed and is approved for publication.



DALE E. CHIMENTI
Nondestructive Evaluation Branch
Metals and Ceramics Division



ROBERT L. CRANE
Nondestructive Evaluation Branch
Metals and Ceramics Division

FOR THE COMMANDER


D. M. FORNEY, JR, CHIEF
Nondestructive Evaluation Branch
Metals and Ceramics Division

"If your address has changed, if you wish to be removed from our mailing list, or if the addressee is no longer employed by your organization please notify AFML/LLP, W-PAFB, OH 45433 to help us maintain a current mailing list".

Copies of this report should not be returned unless return is required by security considerations, contractual obligations, or notice on a specific document.

REPORT DOCUMENTATION PAGE		READ INSTRUCTIONS BEFORE COMPLETING FORM
1. REPORT NUMBER AFML-TR-79-4214	2. GOVT ACCESSION NO.	3. RECIPIENT'S CATALOG NUMBER
4. TITLE (and Subtitle) ELASTIC WAVE PROPAGATION THROUGH MULTILAYERED MEDIA		5. TYPE OF REPORT & PERIOD COVERED Final Report 1 May 1979 - 1 October 1979
		6. PERFORMING ORG. REPORT NUMBER
7. AUTHOR(s) D. E. Chimenti R. L. Crane		8. CONTRACT OR GRANT NUMBER(s) In-House Report
9. PERFORMING ORGANIZATION NAME AND ADDRESS Air Force Materials Laboratory (LLP) AF Wright Aeronautical Laboratories (AFSC) Wright-Patterson Air Force Base, Ohio 45433		10. PROGRAM ELEMENT, PROJECT, TASK AREA & WORK UNIT NUMBERS 6210F; 2418/05/07; WUD-40
11. CONTROLLING OFFICE NAME AND ADDRESS Air Force Materials Laboratory (LLP) AF Wright Aeronautical Laboratories (AFSC) Wright-Patterson Air Force Base, Ohio 45433		12. REPORT DATE March 1980
		13. NUMBER OF PAGES 70
14. MONITORING AGENCY NAME & ADDRESS (if different from Controlling Office)		15. SECURITY CLASS. (of this report) Unclassified
		15a. DECLASSIFICATION/DOWNGRADING SCHEDULE
16. DISTRIBUTION STATEMENT (of this Report) Approved for public release; distribution unlimited.		
17. DISTRIBUTION STATEMENT (of the abstract entered in Block 20, if different from Report)		
18. SUPPLEMENTARY NOTES		
19. KEY WORDS (Continue on reverse side if necessary and identify by block number) Nondestructive Evaluation; Ultrasonics; Elastic Waves; Layered Media <i>wave propagation</i>		
20. ABSTRACT (Continue on reverse side if necessary and identify by block number) This report presents a review of the theory of elastic wave propagation in any number of fluid or solid layered media. Suitable wave equations are derived, and boundary conditions determined by the nature of the media and the character of the interfaces are applied, yielding a formal solution for the transmitted and reflected, longitudinal and transverse wave potentials. Computer-generated graphs are presented which illustrate properties of the solutions in materials of interest in nondestructive evaluation. A tabulation of acoustic-velocity data for media commonly encountered in ultrasonic work is also included.		

FOREWORD

This technical report was prepared by D. E. Chimenti and R. L. Crane of the Nondestructive Evaluation Branch, Metals and Ceramics Division, Air Force Materials Laboratory, Wright-Patterson Air Force Base, Ohio. The research was conducted under Project No. 2418, Task 0507 in Work Unit Directive 40 during the period from May 1979 to October 1979. This report was submitted by the authors in November 1979.

TABLE OF CONTENTS

SECTION		PAGE
I	INTRODUCTION	1
II	SOLUTION OF THE WAVE EQUATIONS	2
	1. Approximations and Assumptions of the Model	2
	2. Wave Equations and the General Solutions	3
	3. An Example	14
III	GRAPHICAL REPRESENTATION OF ENERGY-FLUX COEFFICIENTS FOR SELECTED LAYERED STRUCTURES	16
IV	ACOUSTIC VELOCITY DATA	36
	APPENDIX	59
	REFERENCES	61

LIST OF ILLUSTRATIONS

FIGURE		PAGE
1	Ultrasonic Ray Schematic	6
2	Layer Geometry	7
3	Schematic of Three Layer Structure	15
4a	Longitudinal Wave Incident on a Water/Lucite Interface	17
4b	Longitudinal Wave Incident on a Lucite/Water Interface	17
5a	Longitudinal Wave Incident on an Aluminum/Water Interface	18
5b	Longitudinal Wave Incident on a Steel/Water Interface	18
6a	Longitudinal Wave Incident on an Aluminum/Lucite Interface	19
6b	Longitudinal Wave Incident on a Steel/Lucite Interface	19
7a	Longitudinal Wave Incident on a Beryllium/Lucite Interface	20
7b	Shear Wave Incident on a Beryllium/Lucite Interface	20
8a	Longitudinal Wave Incident on a Beryllium/Steel Interface	21
8b	Longitudinal Wave Incident on a Steel/Beryllium Interface	21
9a	Longitudinal Wave Incident on a Beryllium/Zirconium Interface	22
9b	Longitudinal Wave Incident on a Zirconium/Steel Interface	22
10a	Longitudinal Wave Incident on a Rubber/Steel Interface	23
10b	Shear Wave Incident on a Rubber/Steel Interface	23
11a	Longitudinal Wave Incident on a Steel/Rubber Interface	24
11b	Shear Wave Incident on a Steel/Rubber Interface	24
12a	Longitudinal Wave Incident on a Steel/Quartz Glass Interface	25
12b	Longitudinal Wave Incident on a Quartz Glass/Steel Interface	25
13a	Shear Wave Incident on a Steel/Quartz Glass Interface	26
13b	Shear Wave Incident on a Quartz Glass/Steel Interface	26

LIST OF ILLUSTRATIONS (CONCLUDED)

FIGURE	PAGE
14a Longitudinal Wave Incident on Aluminum/Lucite/Aluminum Structure at 0° and 7.5 MHz	27
14b Longitudinal Wave Incident on Aluminum/Lucite/Aluminum Structure at 5° and 7.5 MHz	27
15a Longitudinal Wave Incident at Aluminum/Lucite/Aluminum Structure at 10° and 7.5 MHz	28
15b Longitudinal Wave Incident on Aluminum/Lucite/Aluminum Structure at 20° and 7.5 MHz	28
16a Longitudinal Wave Incident on Aluminum/Lucite (.026cm)/Aluminum Structure at 7.5 MHz	29
16b Longitudinal Wave Incident on Aluminum/Lucite (.033cm)/Aluminum Structure at 7.5 MHz	29
17a Longitudinal Wave Incident on Aluminum/Lucite (.0355cm)/Aluminum Structure at 7.5 MHz	30
17b Shear Wave Incident on Aluminum/Lucite (.019cm)/Aluminum Structure at 7.5 MHz	30
18a Shear Wave Incident on Aluminum/Lucite/Aluminum Structure at 0° and 7.5 MHz	31
18b Shear Wave Incident on Aluminum/Lucite/Aluminum Structure at 5° and 7.5 MHz	31
19a Shear Wave Incident on Aluminum/Lucite/Aluminum Structure at 10° and 7.5 MHz	32
19b Shear Wave Incident on Aluminum/Lucite/Aluminum Structure at 20° and 7.5 MHz	32
20a Longitudinal Wave Incident on FE/VA/Quartz Structure at 0° and 7.5 MHz	33
20b Longitudinal Wave Incident on FE/VA/Quartz Structure at 5° and 7.5 MHz	33
21a Shear Wave Incident on FE/VA/Quartz Structure at 0° and 7.5 MHz	34
21b Shear Wave Incident on FE/VA (.06cm)/Quartz Structure at 7.5 MHz	34
22 Shear Wave Incident on FE/VA (.07cm)/Quartz Structure at 7.5 MHz	35

SECTION I

INTRODUCTION

The problem of elastic wave propagation in layered media is one of long-standing technological interest. First treated by Rayleigh (Reference 1), it has found application in fields as diverse as seismology, sound insulation, and nondestructive evaluation. The definitive analysis of multilayer sound propagation in solids was performed in 1949 by W. T. Thomson (Reference 2). As indicated recently (Reference 3), Thomson's formulation leads to solutions of limited validity because the shear moduli of all media are assumed to be equal. A completely general analysis, correcting these limitations, is due to Haskell (Reference 4). Earlier, Lindsay (Reference 5) had studied the transmission of elastic waves through alternating fluid and solid layers. Thomson's work was the first, however, to treat the more general problem of propagation in solid layered media. Although the topic has subsequently been discussed at length in several books and review articles (References 6 through 11), it continues to be an area of active research (References 3, 12 through 15). Composite materials and adhesively bonded structures provide examples of layered-media applications of current interest.

Physically, the approach consists of solving suitable wave equations in media for reflected and transmitted longitudinal and transverse waves, subject to boundary conditions determined by the nature of the media and their interfaces. Assumptions concerning the media, interfaces, and wave characteristics allow us to reduce the mathematical complexity of the problem. Nonetheless, the results for all but the simplest cases are algebraically cumbersome, and we present only a formal solution suitable for computer computation, supported by an illustrative example.

Mathematical details of the procedure leading to the solution of the wave equations, subject to appropriate boundary conditions, are presented in the next section. Section III is a collection of graphical solutions for particular media and initial conditions likely to be of interest to the practitioner of nondestructive testing. A tabulation of acoustic data for media commonly encountered in ultrasonic work is the subject of Section IV.

SECTION II

SOLUTION OF THE WAVE EQUATIONS

1. APPROXIMATIONS AND ASSUMPTIONS OF THE MODEL

In this section we specify the problem of wave transmission through layers, outline the simplifying assumptions implicit in the treatment, and proceed stepwise through the solution of the coupled equations to the expressions for the reflected and transmitted wave amplitudes at each interface. The expressions derived at the end of the section have been evaluated by computer and the results used to generate the figures shown in Section IV of this report. Our treatment and notation here follow closely those of earlier work (References 2, 3, 6).

Several important assumptions form the basis for a widely used model of sound wave propagation through solid and liquid layers. Some are more general than others; we consider each in turn. The most important and probably the most general approximation of the model is the assumption of a linearized theory. For a solid, linearity implies the validity of Hooke's Law and allows us to use the principle of superposition and to employ plane-wave trial functions. Further mathematical simplification is achieved by considering only plane waves of infinite aperture and duration. The above approximations do not seriously reduce the validity of the solutions in practical situations so long as the following conditions are met: 1) tone bursts must be long compared to the structure transit time, and 2) spatially-finite acoustic beams can have only a path length through the entire structure which is short with respect to the beam width. Structure refers here to the media contained between the two outermost interfaces. We assume an elastic continuum which leads to linear wave dispersion and neglect the effects of wave attenuation, though these could be easily included in the model. The problem is further particularized by considering only homogeneous, isotropic media separated by plane parallel interfaces, where the media have infinite extent in the x-y plane. Particle motion is assumed to be confined to the x-z plane, reducing the problem to two dimensions. The foregoing assumptions and

approximations are quite common and allow us to simplify the analysis while retaining the applicability of the results to important problems in nondestructive testing.

2. WAVE EQUATIONS AND THE GENERAL SOLUTIONS

The linearized homogeneous wave equation for the particle displacement in an elastic medium is given by Reference 9

$$\rho \ddot{\underline{\xi}} = \mu \nabla^2 \underline{\xi} + (\lambda + \mu) \underline{\nabla} (\underline{\nabla} \cdot \underline{\xi}), \quad (1)$$

where $\underline{\xi}$ is the particle displacement vector, ρ is the mass density, μ and λ are the Lamé constants, and $\nabla^2 \underline{\xi}$ is a vector Laplacian. We use the term particle interchangeably with volume element, which is more appropriate for a fluid or elastic continuum. According to Helmholtz' theorem (Reference 17) we may express the particle velocity vector $\dot{\underline{\xi}}$ ($= d\underline{\xi}/dt$) as the sum of purely irrotational and purely solenoidal vectors as follows.

$$\dot{\underline{\xi}} = \underline{\nabla} \phi + \underline{\nabla} \times \underline{\psi}, \quad (2)$$

where ϕ and $\underline{\psi}$ are potentials corresponding to longitudinal and transverse waves. (Longitudinal waves are also often called compressional, dilational, or P waves, while transverse waves are known alternatively as shear or S waves). If we further assume that the time dependence of $\underline{\xi}$ is harmonic, the particle velocity from Equation 2 becomes $-i\omega \underline{\xi}$, where ω is the frequency and $i \equiv \sqrt{-1}$. In which case, the particle velocity satisfies Equation 1, and the substitution of Equation 2 into Equation 1 may be made. Applying vector identities, reversing the order of differentiation, and collecting terms, we have that

$$[\rho \underline{\nabla} \dot{\phi} - \mu \underline{\nabla} \nabla^2 \phi - (\lambda + \mu) \underline{\nabla} \nabla^2 \phi] + [\rho \underline{\nabla} \times \dot{\underline{\psi}} - \mu \underline{\nabla} \times \nabla^2 \underline{\psi}] = 0 \quad (3)$$

which will be satisfied if the irrotational and solenoidal parts individually vanish. Then the terms in brackets yield separate wave equations for the two potentials,

$$\begin{aligned}\ddot{\phi} &= c^2 \nabla^2 \phi \\ \ddot{\underline{\psi}} &= b^2 \nabla^2 \underline{\psi},\end{aligned}\tag{4}$$

where $c = \sqrt{(\lambda+2\mu)/\rho}$ and $b = \sqrt{\mu/\rho}$ are the longitudinal and transverse wave speeds, respectively. Recalling that in our case particle motion is restricted to the plane of incidence, the vector potential $\underline{\psi}$ need have only a single nonzero component to specify the particle velocity. Explicitly, from Equation 2 we have

$$\begin{aligned}\dot{\xi}_x &= \frac{\partial \phi}{\partial x} - \frac{\partial \psi_y}{\partial z} \\ \dot{\xi}_y &= 0 \\ \dot{\xi}_z &= \frac{\partial \phi}{\partial z} + \frac{\partial \psi_y}{\partial x},\end{aligned}\tag{5}$$

where the subscripts refer to the three spatial coordinate directions. The corresponding stresses are by definition

$$\begin{aligned}\tau_{zx} &= \mu \left(\frac{\partial \xi_x}{\partial z} + \frac{\partial \xi_z}{\partial x} \right) \\ \tau_{yz} &= 0 \\ \tau_{zz} &= \lambda \frac{\partial \xi_x}{\partial x} + (\lambda + 2\mu) \frac{\partial \xi_z}{\partial z},\end{aligned}\tag{6}$$

and these may also be expressed in terms of the wave potentials.

The usual trial solutions for the potentials in any layer which satisfy Equation 4 are

$$\begin{aligned}\phi_{\pm}(\underline{r}, t) &= \Phi_{\pm} \exp i(\underline{k}_{\ell t} \cdot \underline{r} - \omega t) \\ \psi_{\pm}(\underline{r}, t) &= \Psi_{\pm} \exp i(\underline{k}_{t\pm} \cdot \underline{r} - \omega t),\end{aligned}\tag{7}$$

where Φ_{\pm} and Ψ_{\pm} are in general complex potential amplitudes of waves propagating in directions of increasing or decreasing z , according to whether the subscript is + or -. For the position vector \underline{r} , we have that $\underline{r} = x\underline{\hat{e}}_x + y\underline{\hat{e}}_y + z\underline{\hat{e}}_z$, where the $\underline{\hat{e}}$'s are unit vectors along the respective axes. The longitudinal and transverse wavevectors are given respectively by

$$\underline{k}_{\ell\pm} = k_{\ell}(\underline{\hat{e}}_x \sin\theta_{\ell\pm} \pm \underline{\hat{e}}_z \cos\theta_{\ell\pm}) \quad (8)$$

$$\underline{k}_{t\pm} = k_t(\underline{\hat{e}}_x \sin\theta_{t\pm} \pm \underline{\hat{e}}_z \cos\theta_{t\pm}),$$

and $k_{\ell} = |\underline{k}_{\ell\pm}| = \omega/c$, $k_t = |\underline{k}_{t\pm}| = \omega/b$; $\theta_{\ell\pm}$ are the angles of the incident and reflected longitudinal waves as illustrated in Figure 1. At the interface between two layers, indicated in Figure 2, the existence of boundary conditions satisfied at all points on the interface and at all times requires that the phase factors of all the waves at the boundary ($z = 0$) are equal, the exact value being arbitrary (Reference 18). Therefore, we have that

$$\underline{k}_{\ell\pm} \cdot \underline{r} = \underline{k}_{t\pm} \cdot \underline{r} \quad (9)$$

$$\begin{aligned} k_{\ell} \sin\theta_{\ell+} &= k_{\ell} \sin\theta_{\ell-} \\ k_{\ell} \sin\theta_{\ell} &= k_t \sin\theta_t \\ k_{\ell}^{(n)} \sin\theta_{\ell}^{(n)} &= k_{\ell}^{(n-1)} \sin\theta_{\ell}^{(n-1)}, \end{aligned} \quad (9a)$$

where the superscripts in parentheses refer to the layers directly above and below the x -axis in Figure 2. This result is known as Snell's Law in geometrical optics. Parenthetically, the condition expressed in the last line of Equation 9a could, under certain circumstances, lead to values of $\sin\theta_{\ell}^{(n)}$ which were larger than unity. In that case $\theta_{\ell}^{(n)}$ is complex, and the incident wave is totally reflected. Since the choice of n is arbitrary, similar constraints on the phase must exist at every

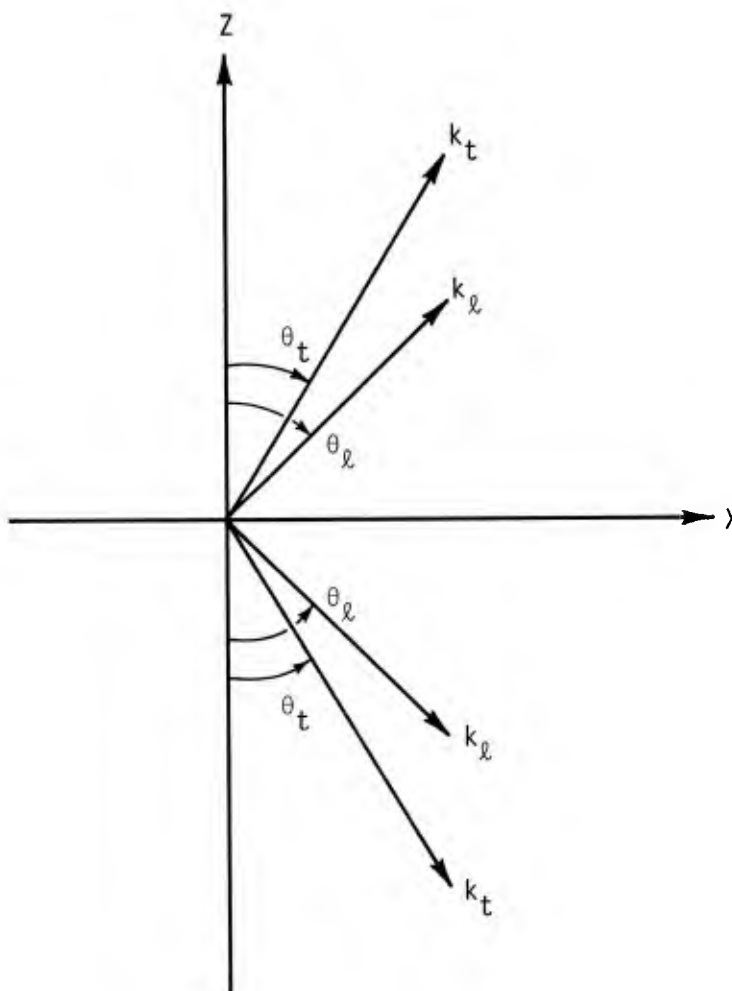


Figure 1. Ultrasonic Ray Schematic

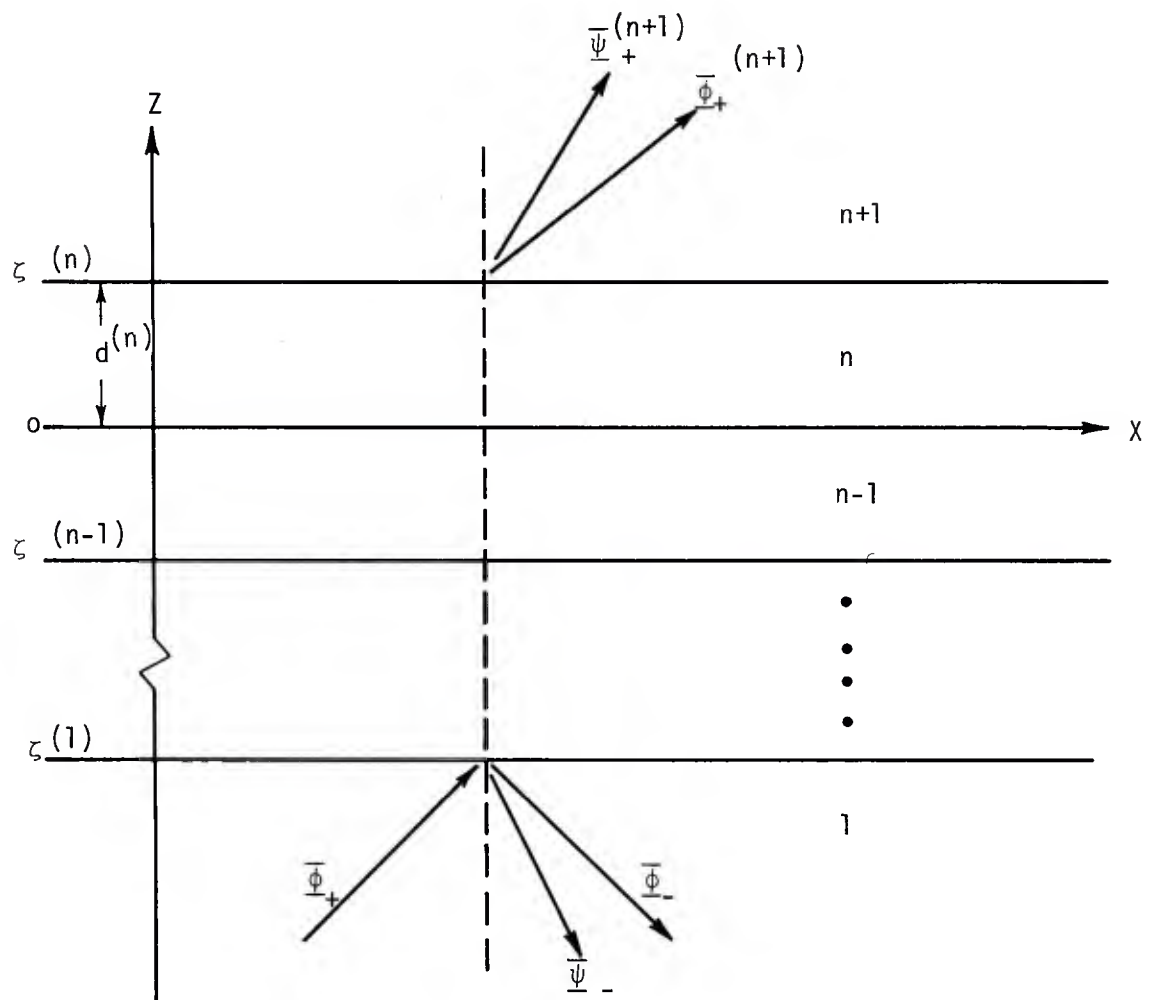


Figure 2. Layer Geometry

interface, and the x-components of the wavevectors will be constant and equal throughout all the media. We express this result by setting $k_{\ell}^{(i)} \sin\theta_{\ell}^{(i)} = k_t^{(i)} \sin\theta_t^{(i)} \equiv q$. The solution of Equation 7 can then be rewritten as follows,

$$\begin{aligned}\phi_{\pm} &= \Phi_{\pm} \exp i(\pm k_{\ell} \cos\theta_{\ell} z) \exp i(qx - \omega t) \\ \psi_{\pm} &= \Psi_{\pm} \exp i(\pm k_t \cos\theta_t z) \exp i(qx - \omega t).\end{aligned}\tag{10}$$

The further restriction that the boundary conditions must hold at all times requires the wave frequency to be constant in all media.

Our plan now is to substitute the above trial functions into the expressions for the particle velocity and stress from Equations 5 and 6, then develop relations between the velocities and stresses and the amplitudes of the wave potentials. Applying suitable boundary conditions, we derive recurrence relations between propagation characteristics in successive layers, leading to a relation between complex wave-potential amplitudes in the first and last media. From these relations, transfer functions of the layered structure are derivable.

Accounting for longitudinal and transverse waves traveling in both the positive and negative z-directions in a single medium, the x-component of the velocity from Equation 5 is

$$\begin{aligned}\dot{\xi}_x &= \Phi_+ i q \exp i(k_{\ell} \cos\theta_{\ell} z + \eta) + \Phi_- i q \exp i(-k_{\ell} \cos\theta_{\ell} z + \eta) \\ &\quad - \Psi_+ i k_t \cos\theta_t \exp i(k_t \cos\theta_t z + \eta) + \Psi_- i k_t \cos\theta_t \exp i(-k_t \cos\theta_t z + \eta),\end{aligned}\tag{11}$$

where $\eta \equiv qx - \omega t$. With the definitions, $\alpha \equiv k_{\ell} \cos\theta_{\ell}$ and $\beta \equiv k_t \cos\theta_t$, expressing the exponentials as sinusoidal functions, and collecting terms, Equation 11 becomes

$$\begin{aligned}\dot{\xi}_x &= \left[i q \cos\alpha z (\Phi_+ + \Phi_-) - q \sin\alpha z (\Phi_+ - \Phi_-) + \beta \sin\beta z (\Psi_+ + \Psi_-) \right. \\ &\quad \left. - i \beta \cos\beta z (\Psi_+ - \Psi_-) \right] e^{i\eta}.\end{aligned}\tag{12}$$

The remaining expressions for the z component of the particle velocity and the stresses may be similarly derived from Equations 5 and 6. Noting that the resulting set of equations is linear in combinations of the wave-potential amplitudes, we may write these equations compactly in matrix form, thusly

$$\begin{pmatrix} \dot{\xi}_x \\ \dot{\xi}_z \\ \tau_{zz} \\ \tau_{zx} \end{pmatrix} = \begin{pmatrix} iq\cos\alpha z & -q\sin\alpha z & -i\beta\cos\beta z & \beta\sin\beta z \\ -\alpha\sin\alpha z & i\alpha\cos\alpha z & -q\sin\beta z & iq\cos\beta z \\ -i\gamma\cos\alpha z & \gamma\sin\alpha z & -i\nu\beta\cos\beta z & \nu\beta\sin\beta z \\ \nu\alpha\sin\alpha z & -i\nu\alpha\cos\alpha z & \gamma\sin\beta z & -i\gamma\cos\beta z \end{pmatrix} \begin{pmatrix} \Phi_+ + \Phi_- \\ \Phi_+ - \Phi_- \\ \Psi_+ - \Psi_- \\ \Psi_+ + \Psi_- \end{pmatrix}, \quad (13)$$

where $\gamma \equiv (\lambda k_\ell^2 + 2\mu\alpha^2)/\omega$ and $\nu \equiv 2\mu q/\omega$. It should be noted that in general α , β , γ , ν , and therefore the displacements, stresses, and potential amplitudes depend on properties of a particular medium. In Equation 13, however, the layer notation has been suppressed for the sake of simplicity. For wave propagation in linear elastic media we require that the particle velocities and stresses be continuous across an interface. To apply these boundary conditions, the expressions on the left-hand side of Equation 13 are evaluated at an interface. Let us consider the nth layer, that is the next-to-the-last medium in a structure having a total of $n + 1$ media. In this layer we evaluate Equation 13 at the upper interface or $z = \xi^{(n)}$, referring to Figure 2. To simplify the matrix algebra, we adopt the following notation.

$$[\underline{\xi}; n] = \begin{pmatrix} \dot{\xi}_x \\ \dot{\xi}_z \\ \tau_{zz} \\ \tau_{zx} \end{pmatrix}, \quad [\Phi; n] = \begin{pmatrix} \Phi_+ + \Phi_- \\ \Phi_+ - \Phi_- \\ \Psi_+ - \Psi_- \\ \Psi_+ + \Psi_- \end{pmatrix},$$

where the second term in brackets n indicates that the column vectors are to be evaluated in the n th medium. Let us further represent the first term on the right in Equation 13 by $\{C;n;z\}$, with the square brackets signifying a column vector, while the braces indicate a 4×4 matrix of coefficients. In these terms, Equation 13 may be rewritten succinctly as

$$[\dot{\xi};n] = \{C;n;\zeta^{(n)}\} [\phi;n] , \quad (14)$$

evaluating the coefficient matrix at the interface between layers n and $n + 1$. In this notation, C identifies the matrix as the one relating velocities and potential amplitudes within the same layer, n is the index of the medium, and the last parameter is the z -coordinate at which the matrix is to be evaluated. We further define $\zeta^{(n)}$ as the coordinate of the interface between layers n and $n + 1$, and the thickness of the n th layer $d^{(n)}$ equals $|\zeta^{(n)} - \zeta^{(n-1)}|$.

A relationship analogous to Equation 14 holds at the n and $n - 1$ interface. Employing the boundary conditions, we equate the velocity-stress column vector just inside medium n with its counterpart in layer $n - 1$ at $z = \zeta^{(n-1)} = 0$. We have that

$$[\dot{\xi};n-1] = \{C;n;0\} [\phi;n] . \quad (15)$$

The wave-potential amplitude vector may be eliminated between Equations 14 and 15 to yield

$$[\dot{\xi};n] = \{C;n;d^{(n)}\} \{C;n;0\}^{-1} [\dot{\xi};n-1] , \quad (16)$$

where the superscript -1 on the second coefficient matrix indicates inversion. If we now define the product of the square matrices in Equation 16 by $\{T;n\}$, whose elements are given explicitly in the Appendix, a recurrence relation among velocity-stress vectors in various

layers can be developed by suitably transforming the origin of coordinates and successively applying Equation 16. The resulting equation is

$$[\underline{\xi};n] = \{T;n\} \{T;n-1\} \cdots \{T;2\} [\underline{\xi};1] \quad (17)$$

which constitutes the formal solution of Equation 1 subject to boundary conditions appropriate for sound propagation through multi-layered media. Previous treatments (References 2, 3, 6) terminate the formal analysis at this point. However, with two additional transformations, this solution may be cast in a form directly applicable to the evaluation of experimentally useful quantities. Substituting for the velocity-stress column vector from Equation 14 yields a relationship between the wave-potential amplitudes in the first and the nth media. We have that

$$[\phi;n] = \{C;n;\zeta^{(n)}\}^{-1} \prod_{\ell=n}^2 \{T;\ell\} \{C;1;\zeta^{(1)}\} [\phi;1] , \quad (18)$$

where the product of the $\{T;\ell\}$ matrices is indicated by the symbol Π .

By applying the usual continuity condition to the velocity-stress vector at $z = \zeta^{(n)}$, we have from Equation 14

$$[\phi;n+1] = \{C;n+1;\zeta^{(n)}\}^{-1} \{C;n;\zeta^{(n)}\} [\phi;n] . \quad (19)$$

If we now substitute for the third term on the right hand side of Equation 19 and cancel where possible, the solution may be expressed in its final form:

$$[\phi;n+1] = \{C;n+1;\zeta^{(n)}\}^{-1} \prod_{\ell=n}^2 \{T;\ell\} \{C;1;\zeta^{(1)}\} [\phi;1] . \quad (20)$$

Equation 20 expresses the wave-potential amplitudes in the last or exit medium in terms of those in the entrance medium and is directly applicable to the calculation of energy-flux transfer coefficients, which is pursued below. One should bear in mind that Equation 20 represents, in the most general case, four linear equations in four unknowns. These variables are the amplitudes $\phi_+^{(n+1)}$, $\psi_+^{(n+1)}$, $\phi_-^{(1)}$, and $\psi_-^{(1)}$. Of the remaining

wave-potential amplitudes $\phi_+^{(1)}$ and $\psi_+^{(1)}$ are incident waves determined by initial conditions, whereas $\phi_-^{(n+1)}$ and $\psi_-^{(n+1)}$ are identically zero. For all but the simplest layered structures, Equation 20 leads to very complicated algebraic expressions. However, it is readily adaptable to computer analysis.

We may now proceed to derive expressions for transmitted and reflected power density. Since there will generally be mode conversion of the incident wave, it is of interest to calculate separate power transfer coefficients for longitudinal and transverse modes. The rms acoustic power per unit area has the following mechanical definition,

$$P = \frac{1}{2} \rho s |\dot{\xi}|^2, \quad (21)$$

where s is the wave speed, and ρ is the mass density. From Equation 5 the particle velocity $\dot{\xi}$ may be expressed in terms of the wave-potential amplitudes and these in turn inserted into Equation 21 to yield power transfer coefficients. Relating wave-potential amplitudes in the first and last media is accomplished by combining Equations 14 and 21, eliminating the velocity-stress column vector from the latter equation. If a purely longitudinal wave is incident from below upon a layered structure, as in Figure 2, the incident power in the longitudinal mode will be, according to Equations 5, 7, and 21,

$$\begin{aligned} P_{\ell+} &= \frac{1}{2} \rho c \left[|iq\phi_+|^2 + |ik_{\ell} \cos \theta_{\ell} \phi_+|^2 \right] \\ &= \frac{1}{2} \rho c |k_{\ell}|^2 |\phi_+|^2, \end{aligned} \quad (22)$$

where the $\ell+$ subscripts refer to incident longitudinal power. The layer notation has been suppressed in Equation 22 to improve readability, though medium 1 is clearly implied. The longitudinal power transmitted into the last medium, $n+1$, is given by

$$P_{\ell+}^{(n+1)} = \frac{1}{2} \rho^{(n+1)} c^{(n+1)} |k_{\ell}^{(n+1)}|^2 |\phi_+^{(n+1)}|^2, \quad (23)$$

and the normalized transmitted longitudinal power per unit area or energy-flux coefficient is therefore

$$T_{\ell\ell} = \frac{\rho^{(n+1)} c^{(n+1)} |k_{\ell}^{(n+1)}|^2 |\Phi_+^{(n+1)}|^2 \cos\theta_{\ell}^{(n+1)}}{\rho^{(1)} c^{(1)} |k_{\ell}^{(1)}|^2 |\Phi_+^{(1)}|^2 \cos\theta_{\ell}^{(1)}} , \quad (24)$$

where the $\cos\theta$ factors account for the geometrical variation in the areal power density as the wave is refracted at an interface. Further formal energy-flux transfer coefficients for transverse mode waves are similarly derived. The transmitted and reflected energy-flux coefficients for transverse waves, assuming incident longitudinal waves, are given respectively by

$$T_{\ell t} = \frac{\rho^{(n+1)} b^{(n+1)} |k_t^{(n+1)}|^2 |\Psi_+^{(n+1)}|^2 \cos\theta_t^{(n+1)}}{\rho^{(1)} c^{(1)} |k_{\ell}^{(1)}|^2 |\Phi_+^{(1)}|^2 \cos\theta_{\ell}^{(1)}} \quad (25)$$

$$R_{\ell t} = \frac{b^{(1)} |k_t^{(1)}|^2 |\Psi_-^{(1)}|^2 \cos\theta_t^{(1)}}{c^{(1)} |k_{\ell}^{(1)}|^2 |\Phi_+^{(1)}|^2 \cos\theta_{\ell}^{(1)}} .$$

An additional piece of information of some utility is the phase of the reflected and transmitted wave amplitudes relative to the phase of the incident waveform. For a transmitted longitudinal wave, the relative phase is

$$\phi_{\ell t}^{(n+1)} = \tan^{-1} \frac{\text{Im} \left[k_{\ell}^{(n+1)} \Phi_+^{(n+1)} \right]}{\text{Re} \left[k_{\ell}^{(n+1)} \Phi_+^{(n+1)} \right]} , \quad (26)$$

where Re and Im denote the real and imaginary parts of the expression in parentheses, and \tan^{-1} is the arctangent.

3. AN EXAMPLE

As an example of the foregoing analysis, let us consider propagation through a solid plate immersed in a fluid medium. In that case only longitudinal waves will be present in the entrance and exit media, as shown in Figure 3. We postulate a longitudinal wave incident on medium 2, a solid layer, from medium 1. Equation 20 then tells us how to relate wave-potential amplitudes in the entrance and exit media. We have

$$[\phi;3] = \{C;3;d^{(2)}\}^{-1}\{T;2\}\{C;1;0\} [\phi;1], \quad (27)$$

where it is understood that the potential amplitudes corresponding to transverse waves vanish in media 1 and 3. Expressing the product of square matrices on the right-hand-side of Equation 26 by Q_{ij} , and writing out the amplitude vectors yields

$$\begin{pmatrix} \phi_+^{(3)} \\ \phi_+^{(3)} \\ 0 \\ 0 \end{pmatrix} = Q_{ij} \begin{pmatrix} \phi_+ + \phi_- \\ \phi_+ - \phi_- \\ 0 \\ 0 \end{pmatrix}, \quad (28)$$

where the superscript designating medium 1 has been suppressed. Writing out components, we obtain

$$\begin{aligned} \phi_+^{(3)} &= Q_{11}(\phi_+ + \phi_-) + Q_{12}(\phi_+ - \phi_-) \\ \phi_+^{(3)} &= Q_{21}(\phi_+ + \phi_-) + Q_{22}(\phi_+ - \phi_-). \end{aligned} \quad (29)$$

When $\phi_+^{(3)}$ is eliminated, we have

$$\phi_- = \frac{Q_{11} + Q_{12} - Q_{21} - Q_{22}}{Q_{12} + Q_{21} - Q_{11} - Q_{22}} \phi_+ \quad (30)$$

which may be inserted into an expression similar to Equation 25 to obtain the reflected power density. The transmitted power density is likewise obtained by solving Equations 28 and 29 for $\phi_+^{(3)}$ and substituting the result into Equation 24.

In this section we have specified the problem of wave propagation through layered media, presented and justified simplifying assumptions, and approximations, derived a method to solve the m-layer problem, and exhibited formal expressions for the energy flux transfer coefficients. With these results we proceed, in the following section, to demonstrate the characteristics of these solutions in various circumstances of practical interest.

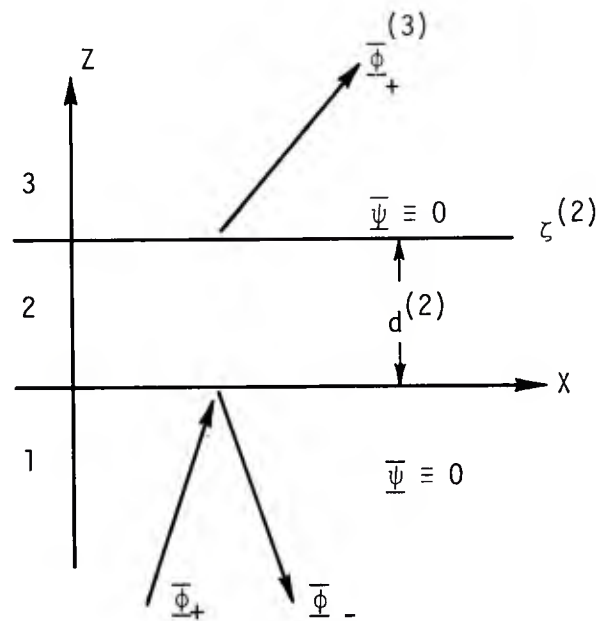


Figure 3. Schematic of Three Layer Structure

SECTION III

GRAPHICAL REPRESENTATION OF ENERGY-FLUX COEFFICIENTS
FOR SELECTED LAYERED STRUCTURES

The following curves are presented as concrete examples of the analysis of Section II. They demonstrate the strong dependence of wave transmission on angle of incidence, layer thickness, and material properties and provide useful insights concerning the effects of mode conversion at interfaces. A computer program based on Equation 20 is employed to calculate the relevant energy-flux coefficients and their phases relative to the incident wave. These results are then plotted as a function of angle of incidence. In the examples treating three media, the dependence on acoustic wavelength is also shown. In general, the configurations selected for analysis have been chosen with a view toward known or potential problems of interest in nondestructive testing.

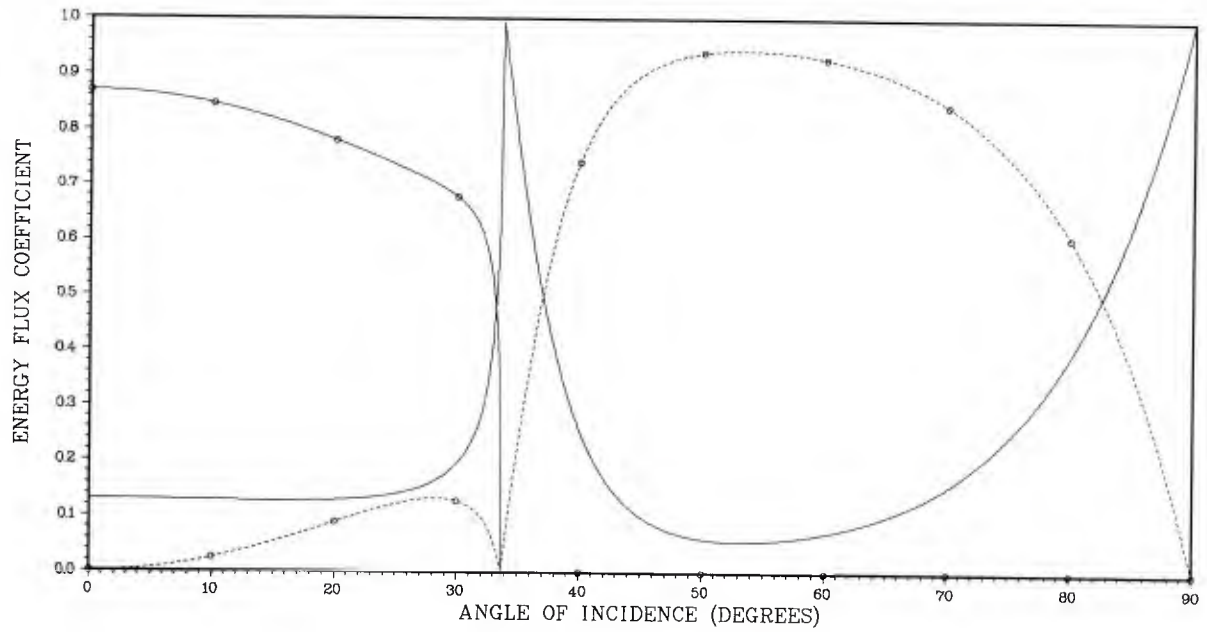


Figure 4a. Longitudinal Wave Incident on a Water/Lucite Interface

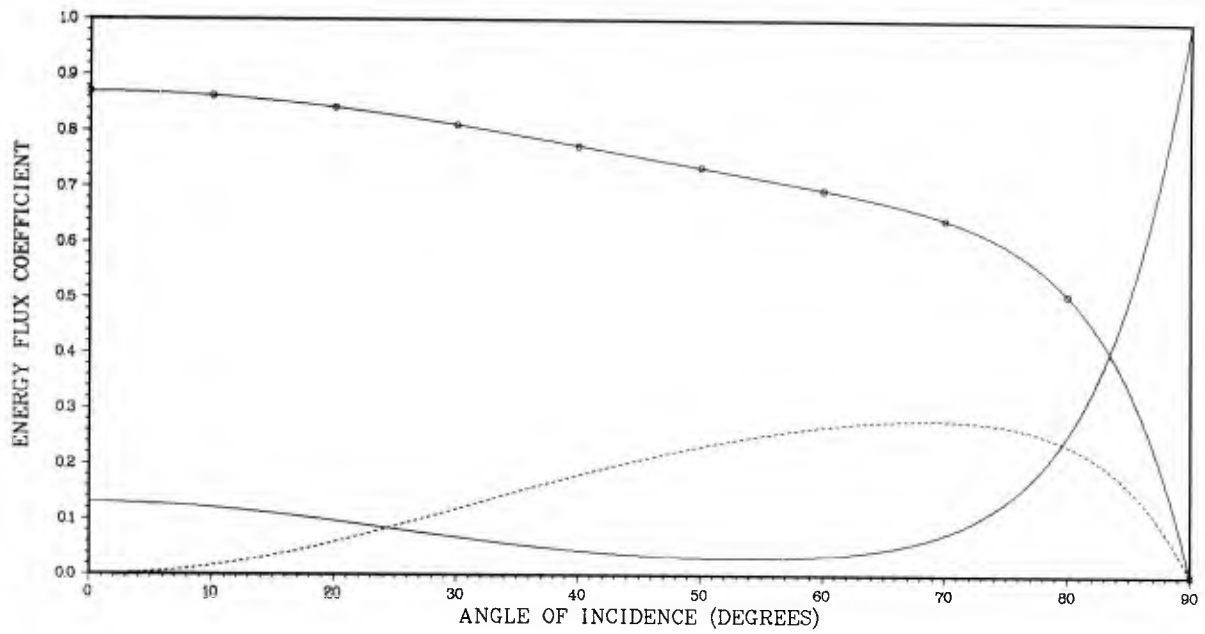


Figure 4b. Longitudinal Wave Incident on a Lucite/Water Interface

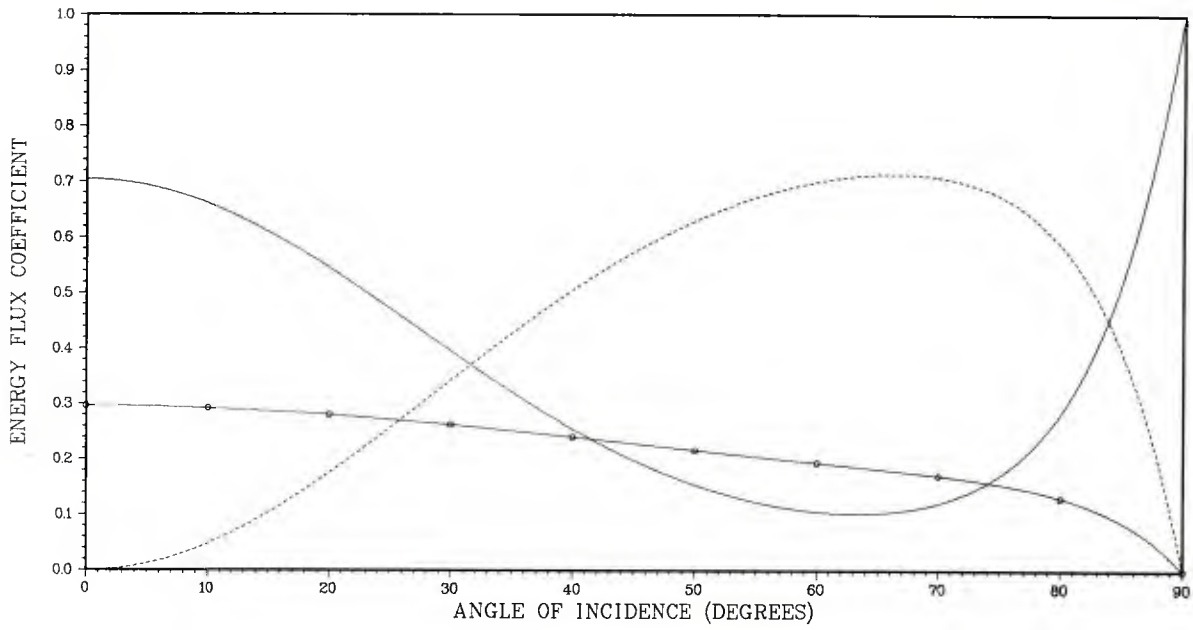


Figure 5a. Longitudinal Wave Incident on an Aluminum/Water Interface

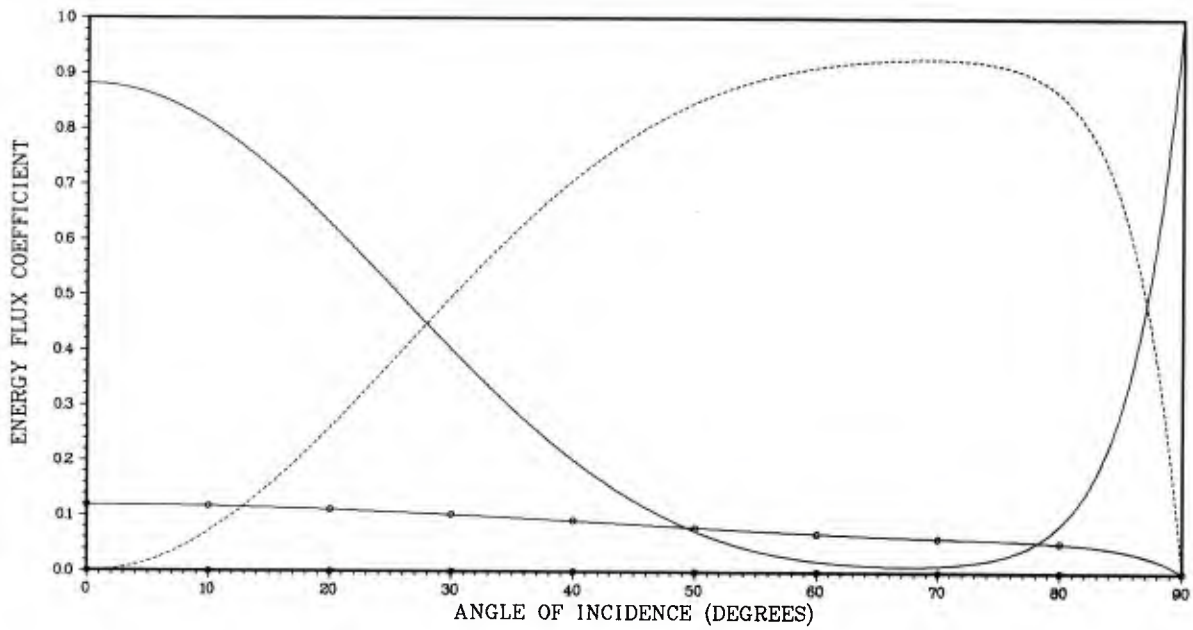


Figure 5b. Longitudinal Wave Incident on a Steel/Water Interface

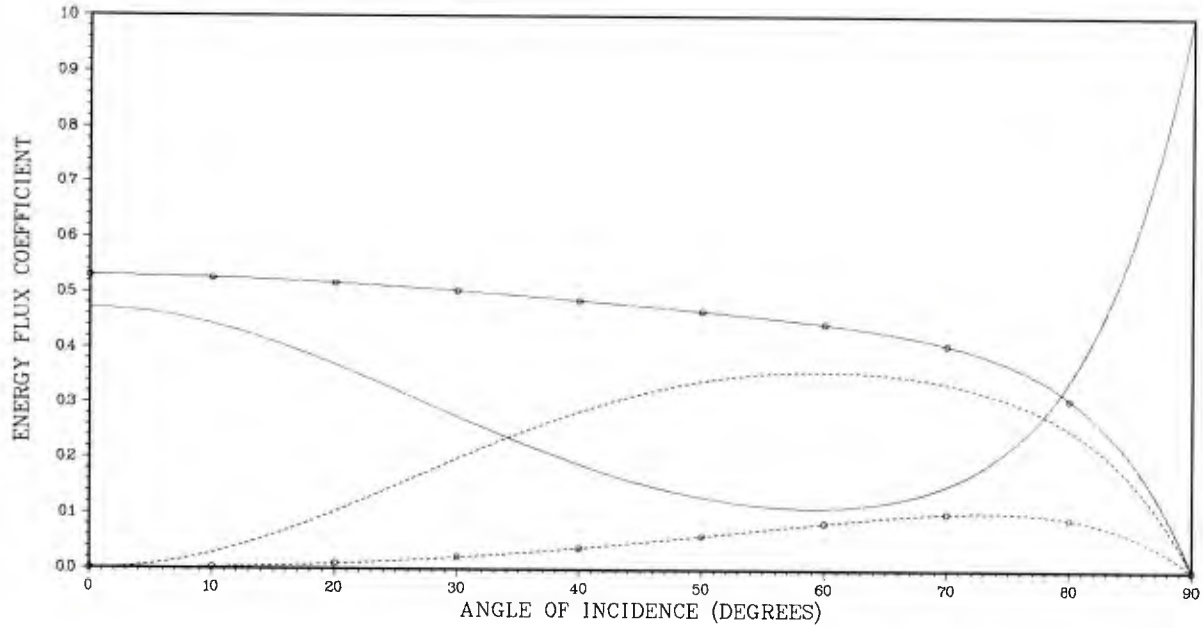


Figure 6a. Longitudinal Wave Incident on an Aluminum/Lucite Interface

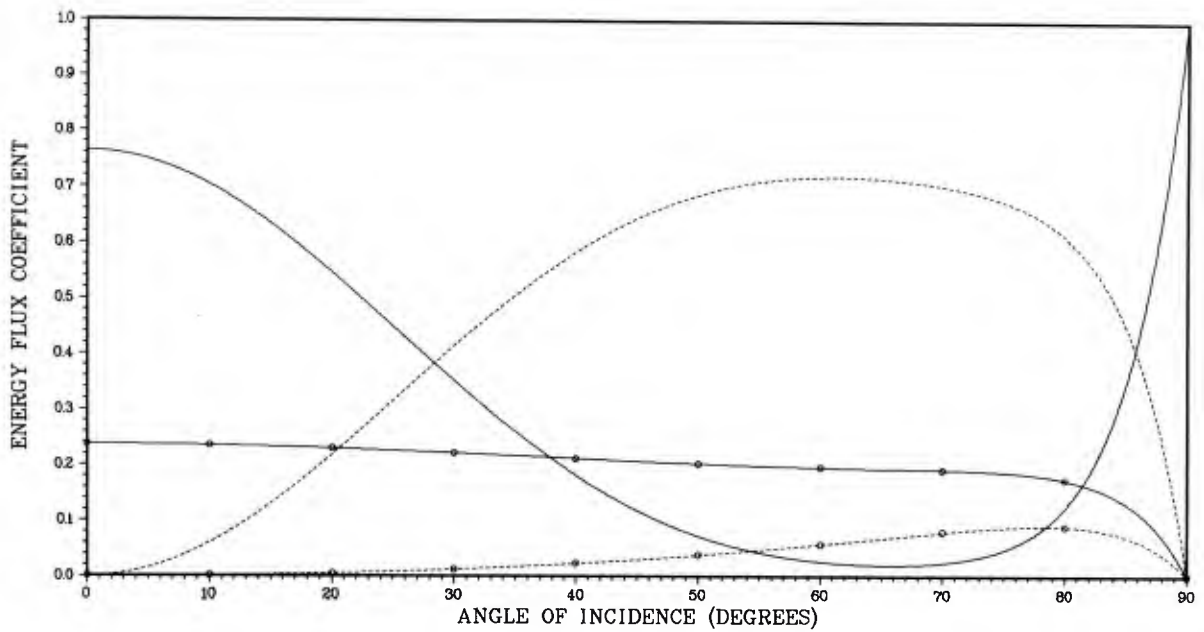


Figure 6b. Longitudinal Wave Incident on a Steel/Lucite Interface

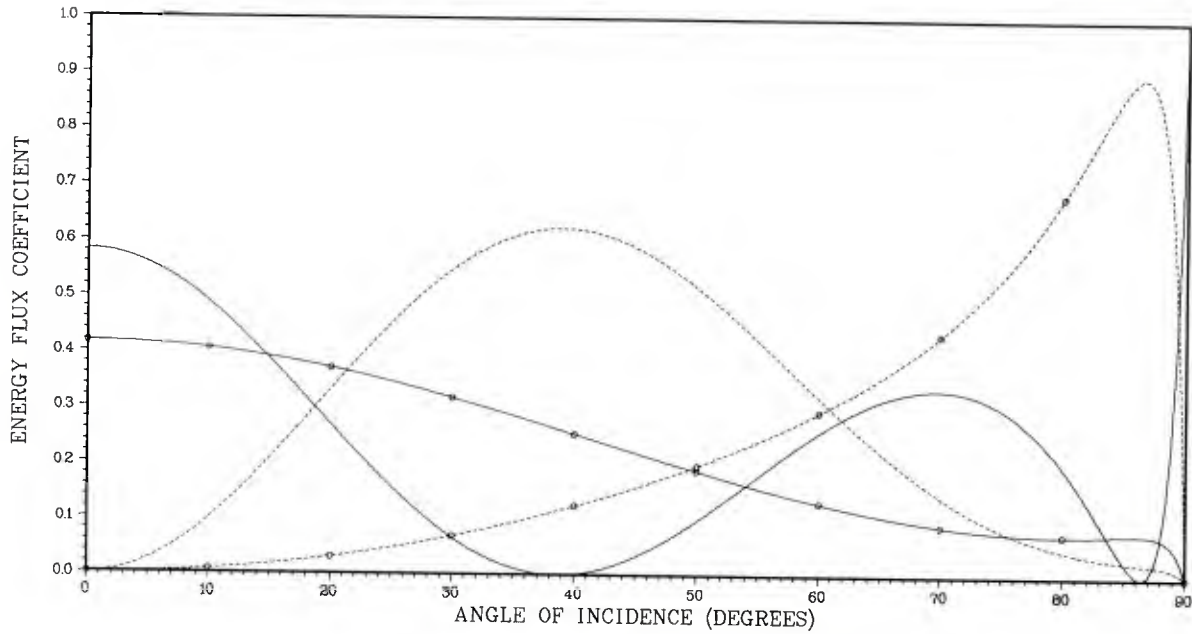


Figure 7a. Longitudinal Wave Incident on a Beryllium/Lucite Interface

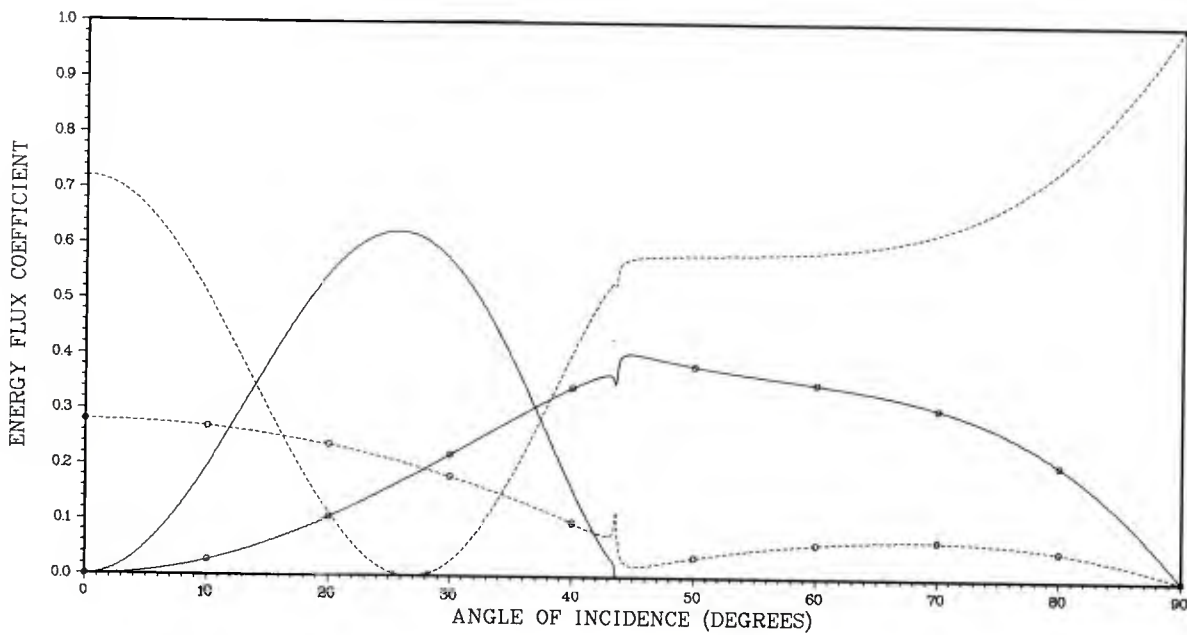


Figure 7b. Shear Wave Incident on a Beryllium/Lucite Interface

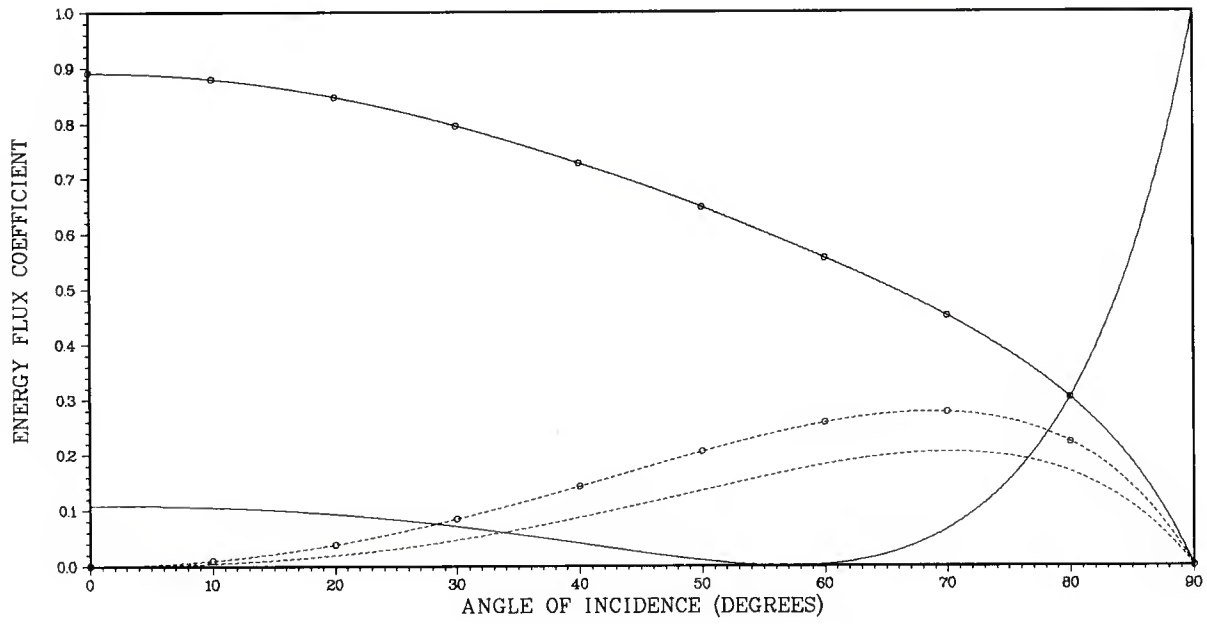


Figure 8a. Longitudinal Wave Incident on a Beryllium/Steel Interface

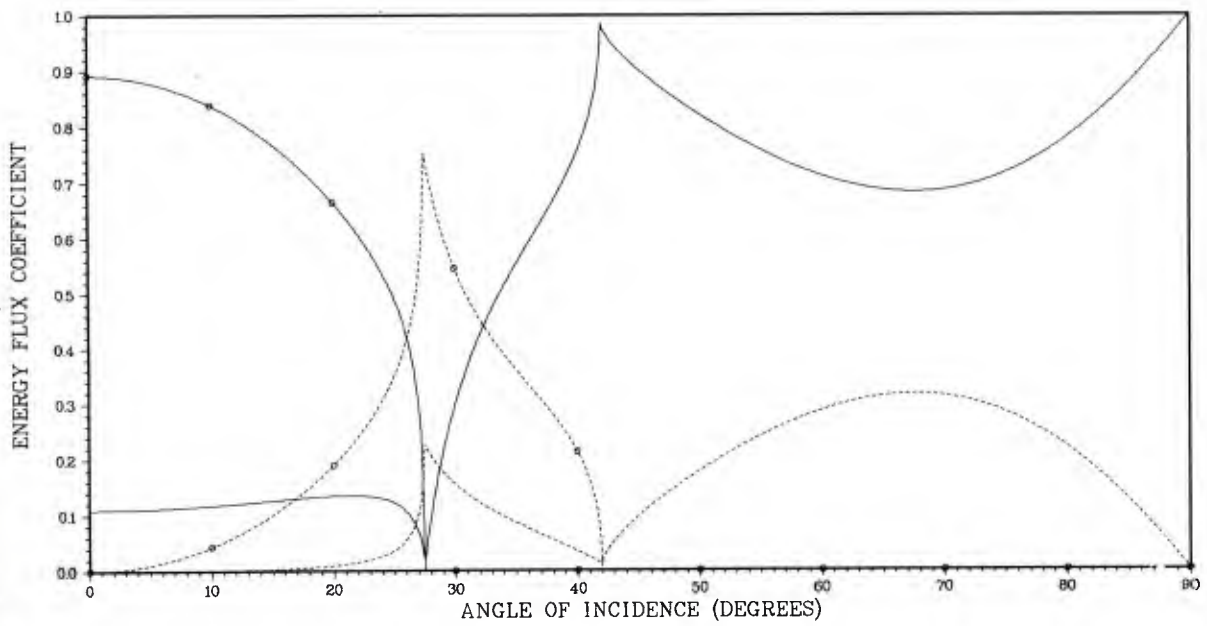


Figure 8b. Longitudinal Wave Incident on a Steel/Beryllium Interface

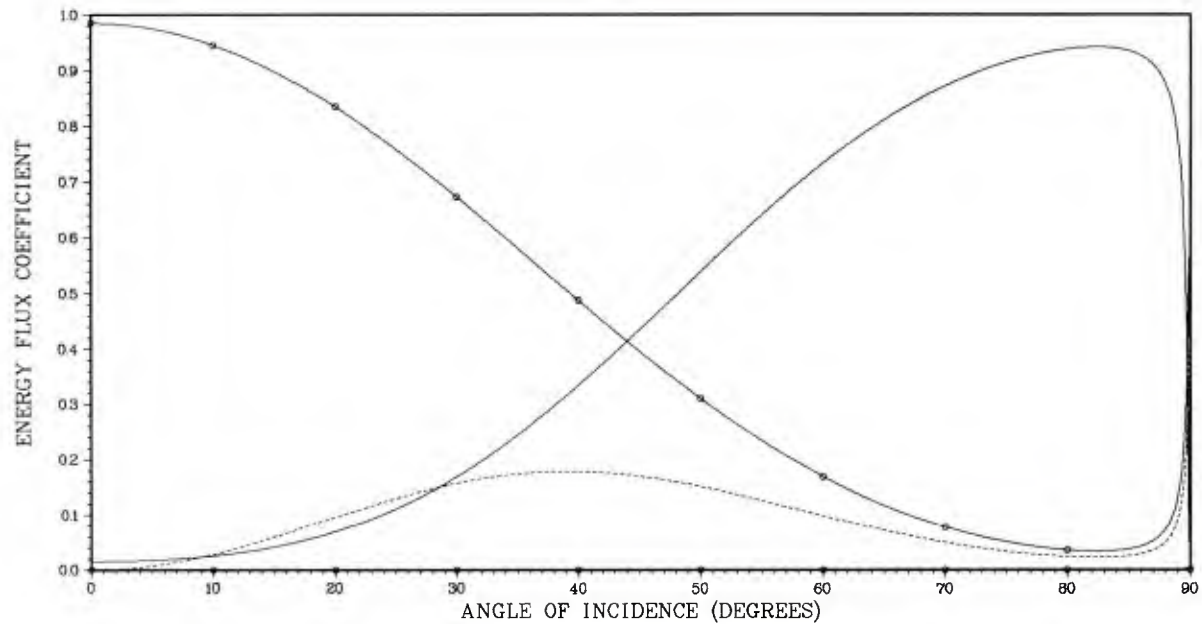


Figure 9a. Longitudinal Wave Incident on a Beryllium/Zirconium Interface

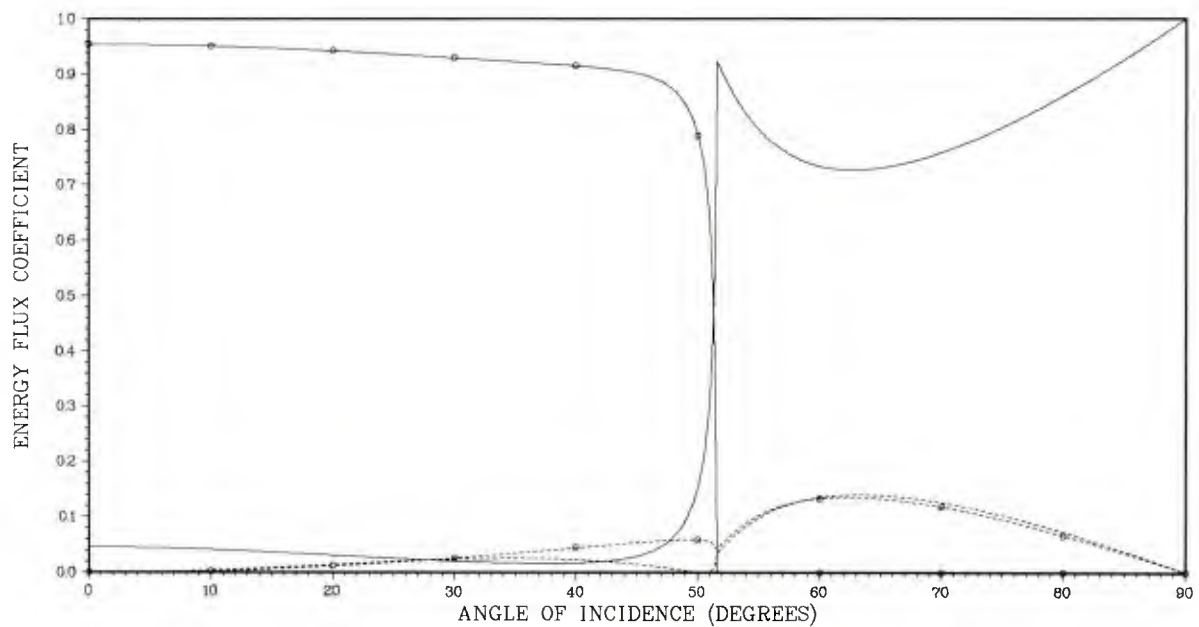


Figure 9b. Longitudinal Wave Incident on a Zirconium/Steel Interface

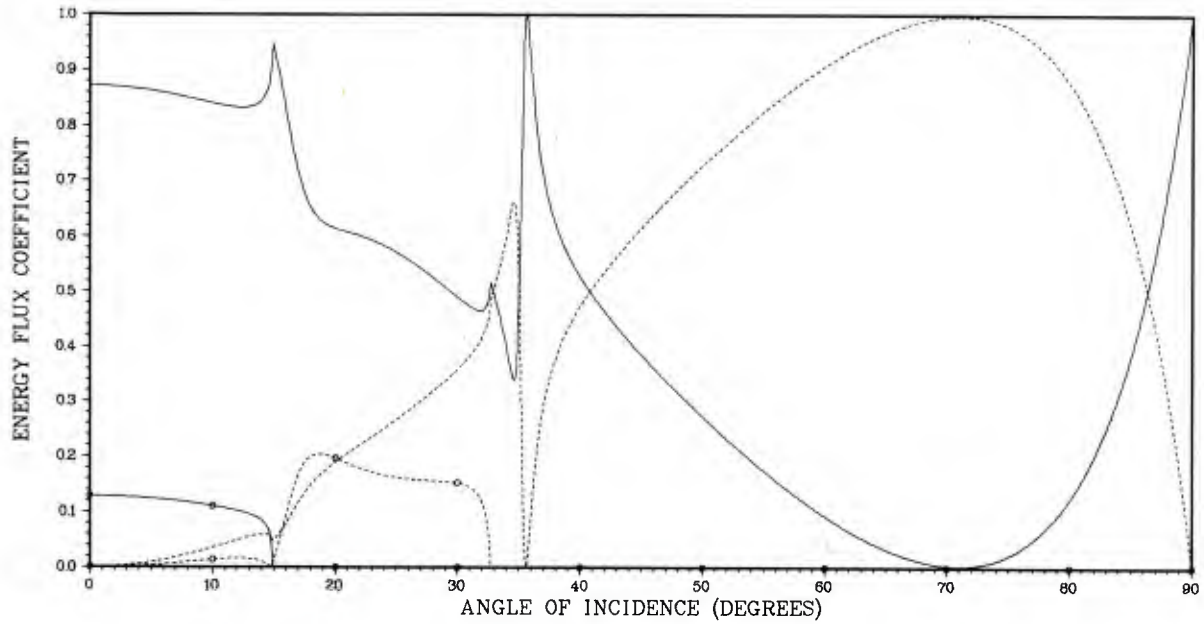


Figure 10a. Longitudinal Wave Incident on a Rubber/Steel Interface

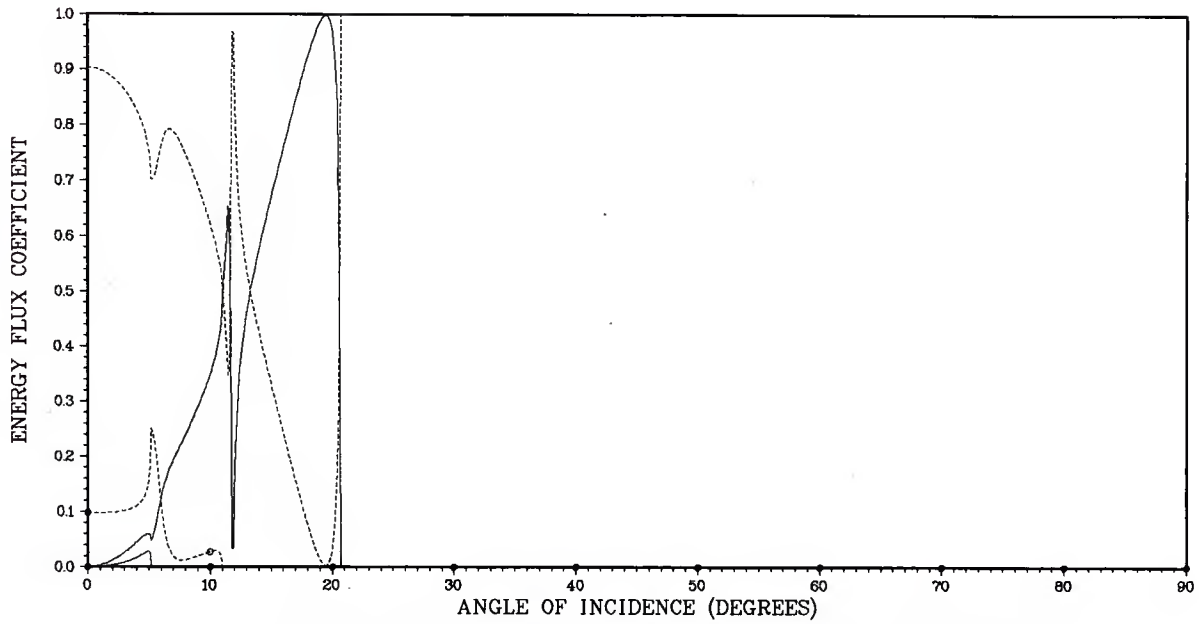


Figure 10b. Shear Wave Incident on a Rubber/Steel Interface

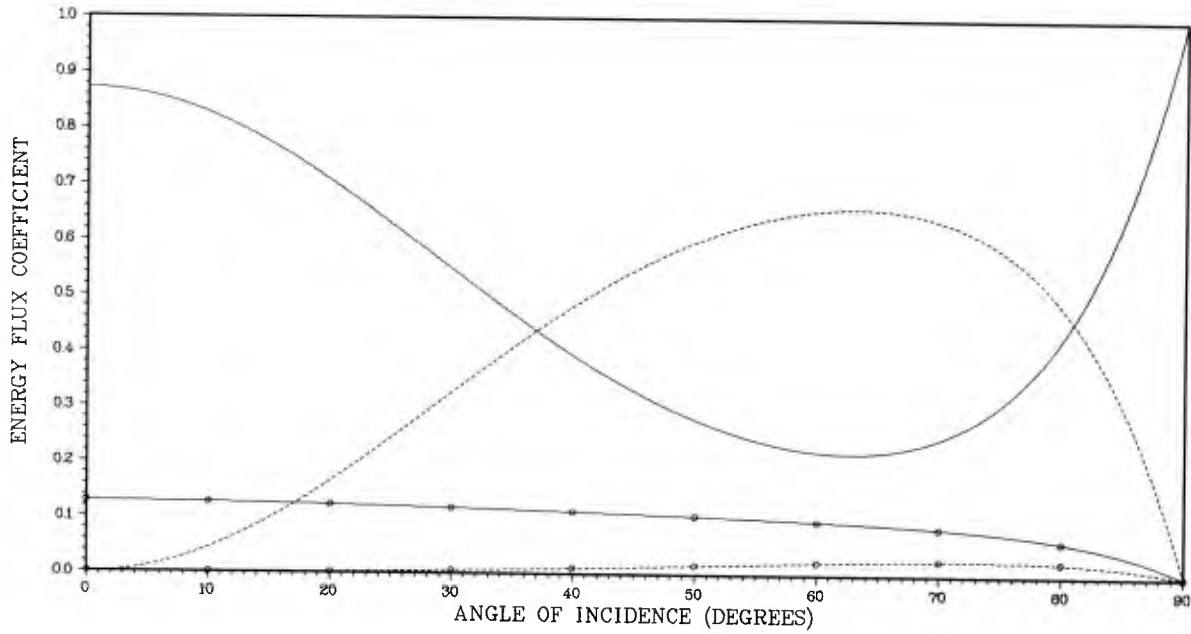


Figure 11a. Longitudinal Wave Incident on a Steel/Rubber Interface

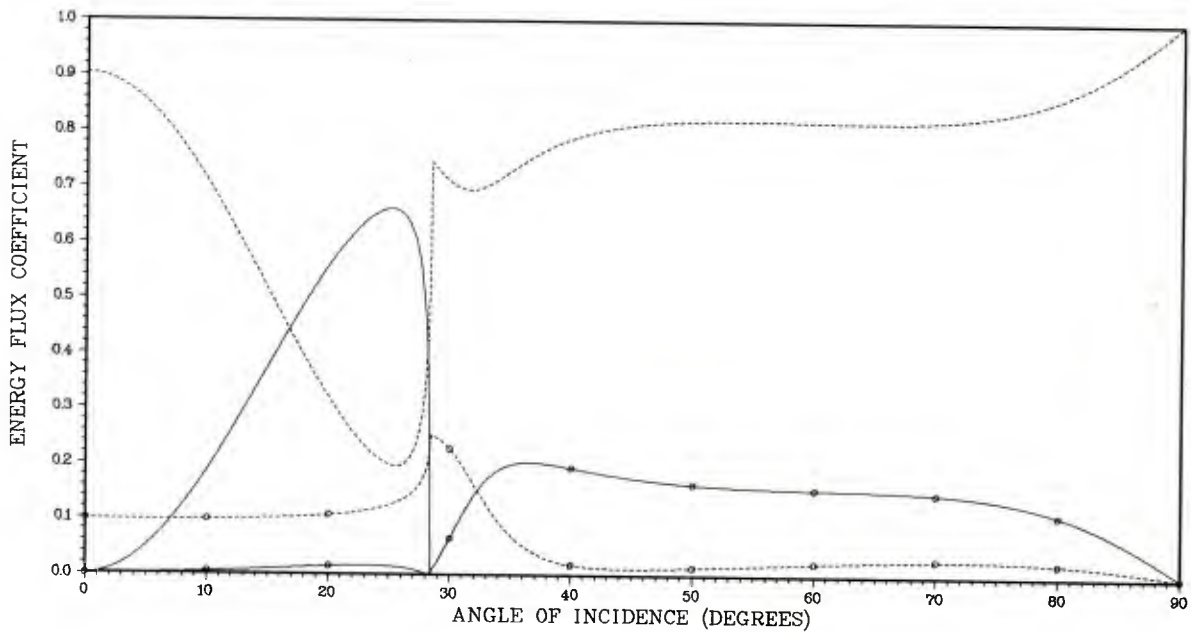


Figure 11b. Shear Wave Incident on a Steel/Rubber Interface

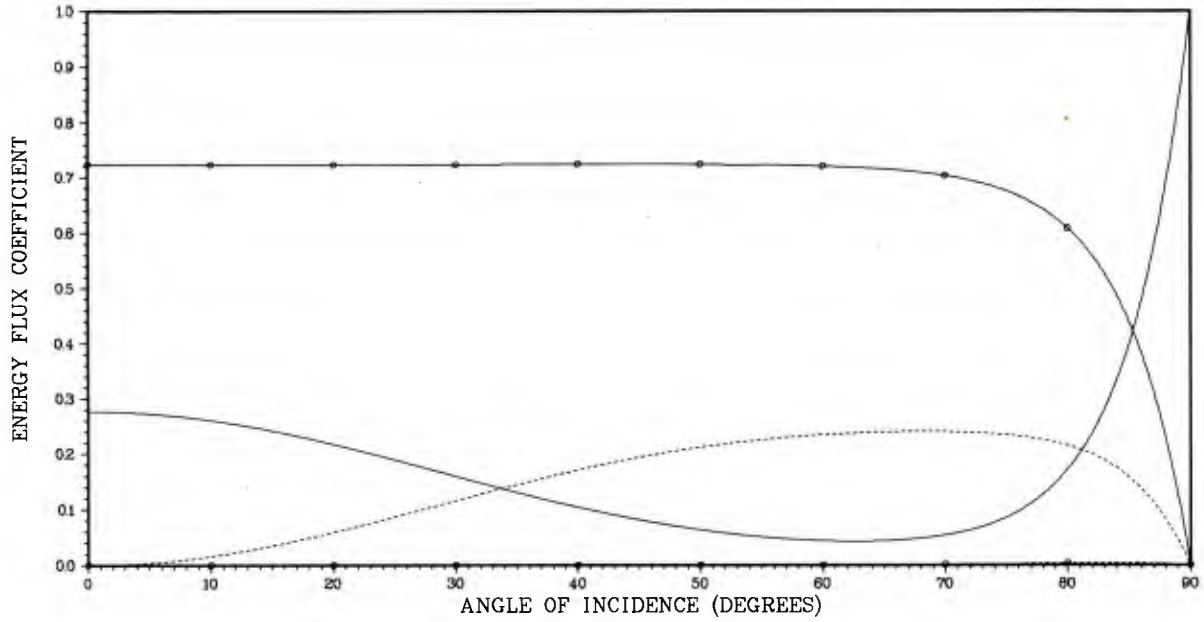


Figure 12a. Longitudinal Wave Incident on a Steel/Quartz Glass Interface

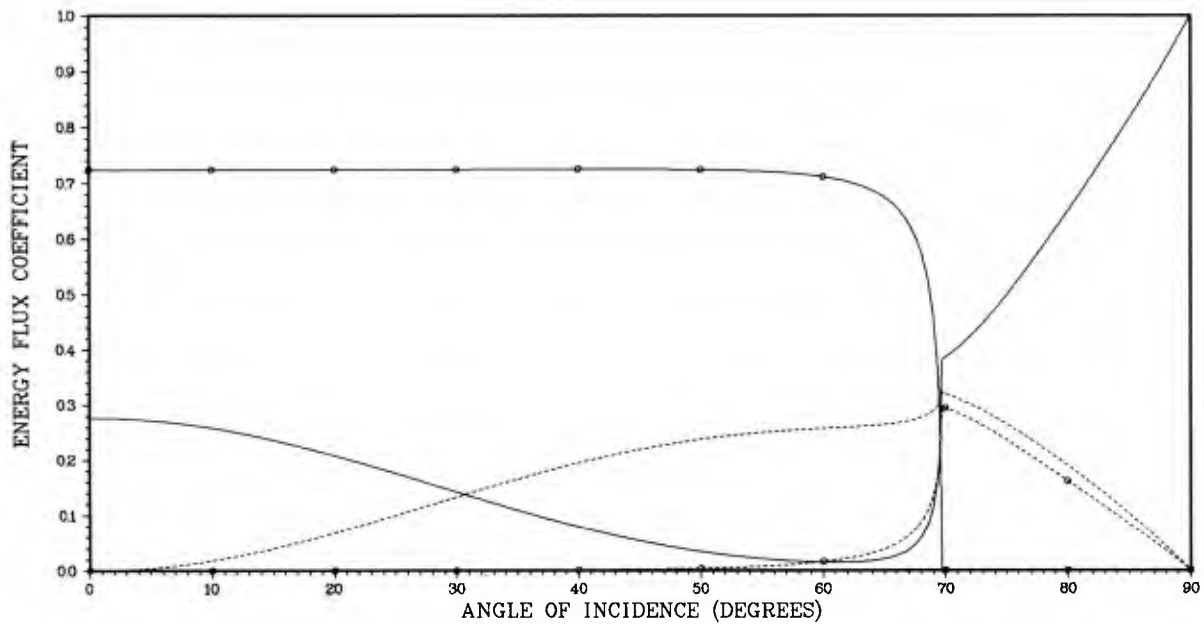


Figure 12b. Longitudinal Wave Incident on a Quartz Glass/Steel Interface

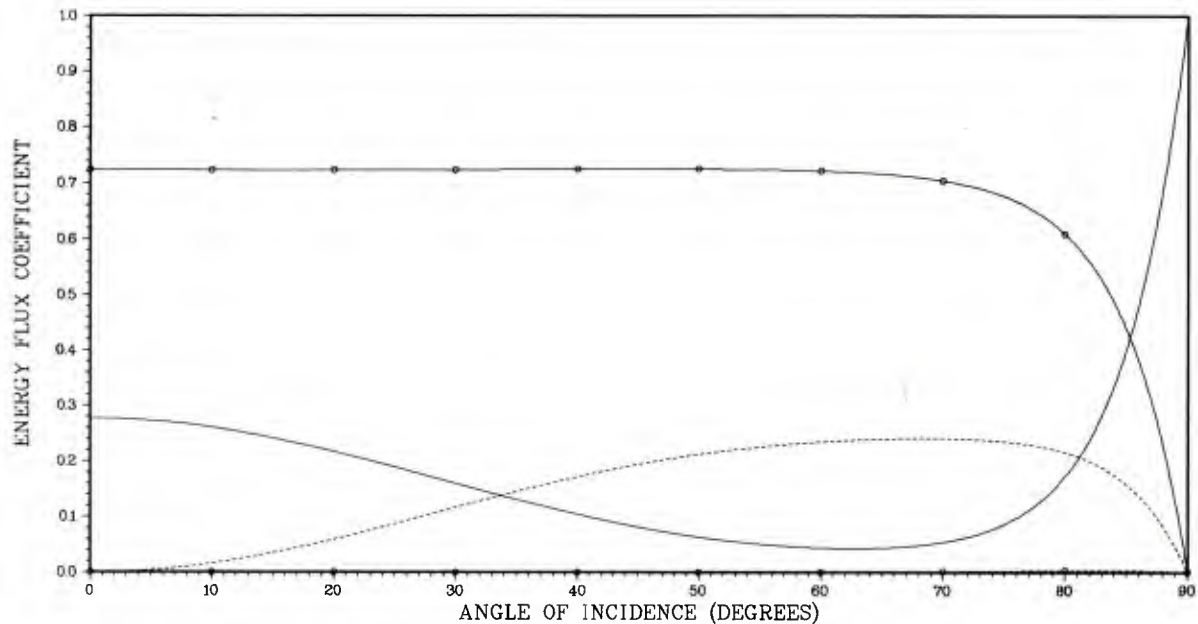


Figure 13a. Shear Wave Incident on a Steel/Quartz Glass Interface

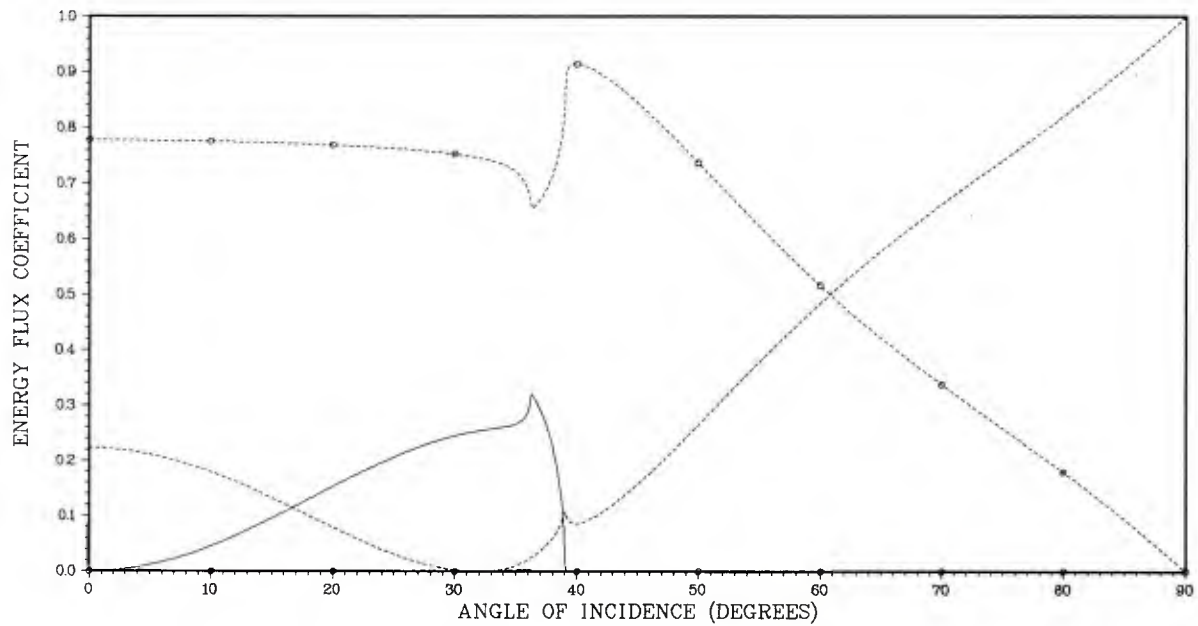


Figure 13b. Shear Wave Incident on a Quartz Glass/Steel Interface

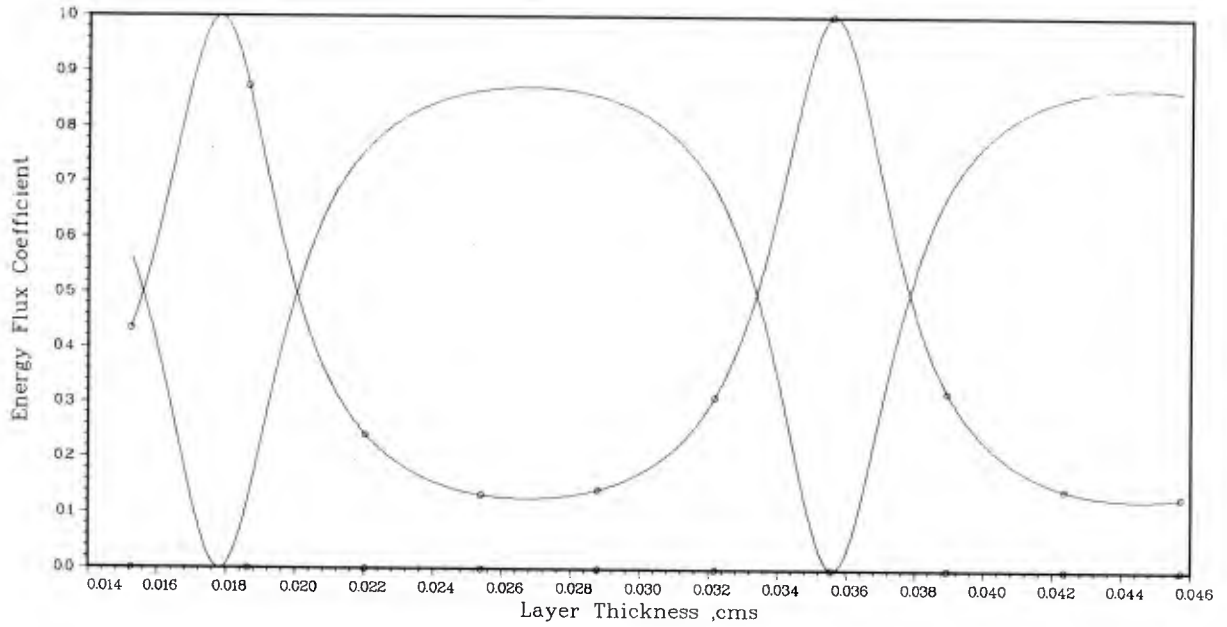


Figure 14a. Longitudinal Wave Incident on Aluminum/Lucite/Aluminum Structure at 0° and 7.5 MHz

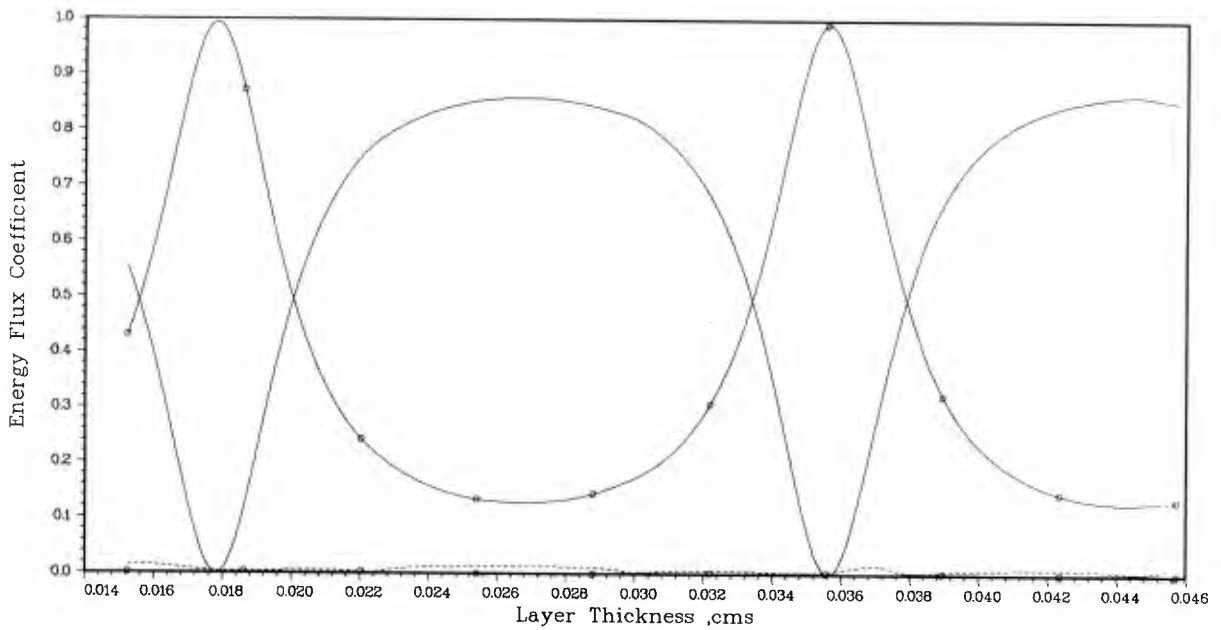


Figure 14b. Longitudinal Wave Incident on Aluminum/Lucite/Aluminum Structure at 5° and 7.5 MHz

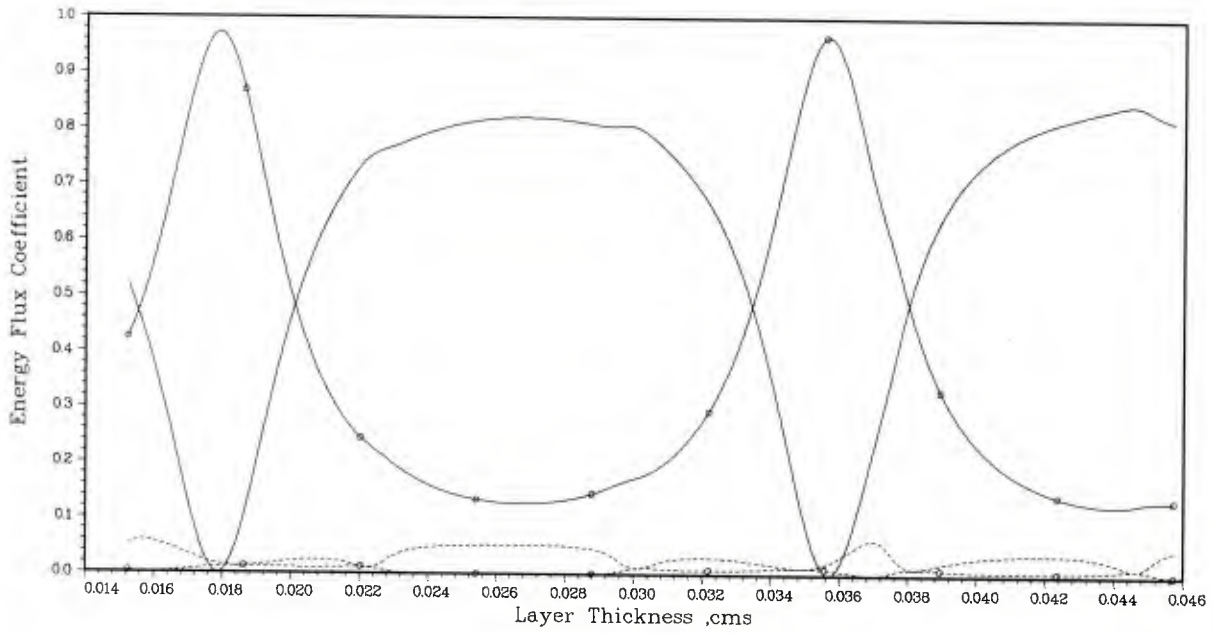


Figure 15a. Longitudinal Wave Incident at Aluminum/Lucite/Aluminum Structure at 10° and 7.5 MHz

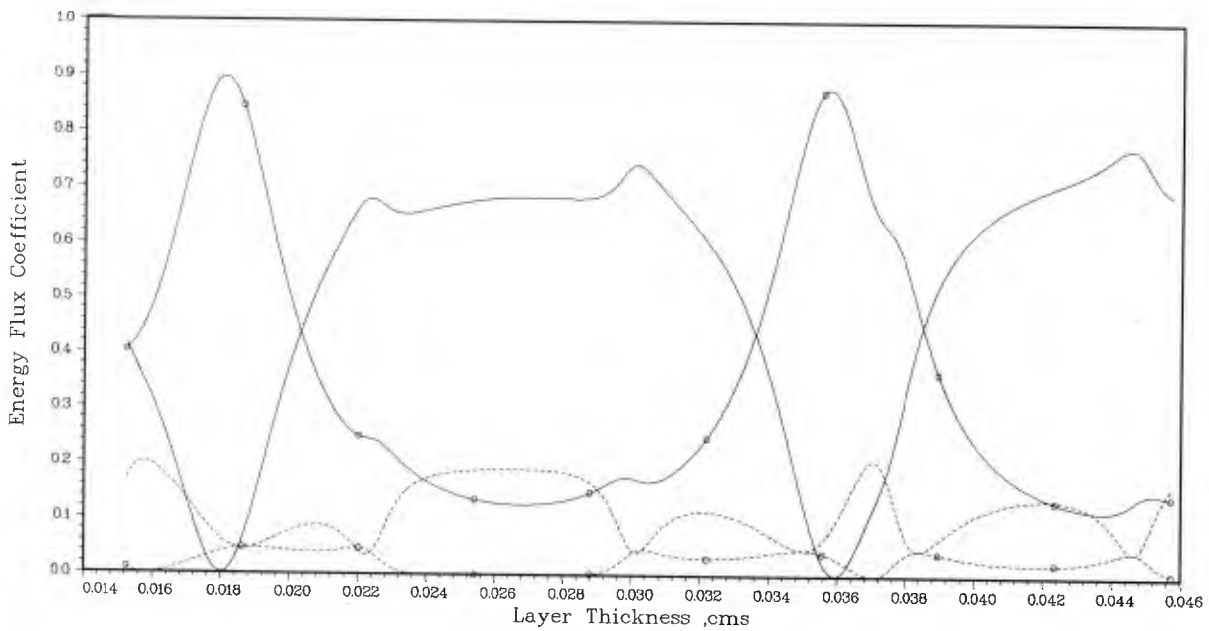


Figure 15b. Longitudinal Wave Incident on Aluminum/Lucite/Aluminum Structure at 20° and 7.5 MHz

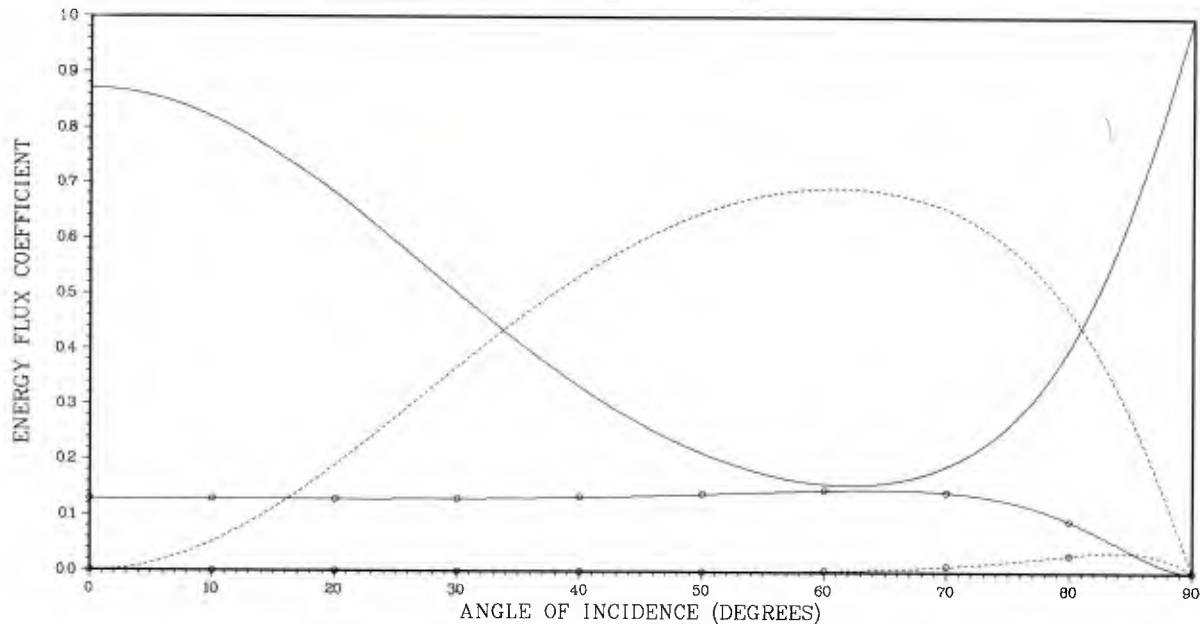


Figure 16a. Longitudinal Wave Incident on Aluminum/Lucite (.026cm)/ Aluminum Structure at 7.5 MHz

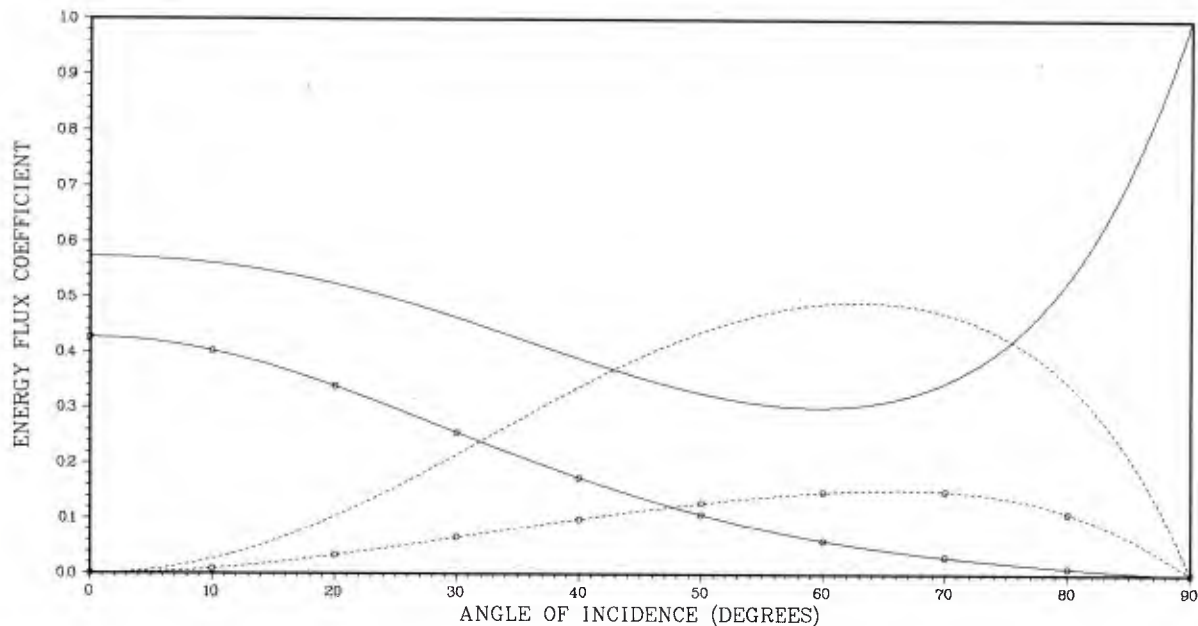


Figure 16b. Longitudinal Wave Incident on Aluminum/Lucite (.033cm)/ Aluminum Structure at 7.5 MHz

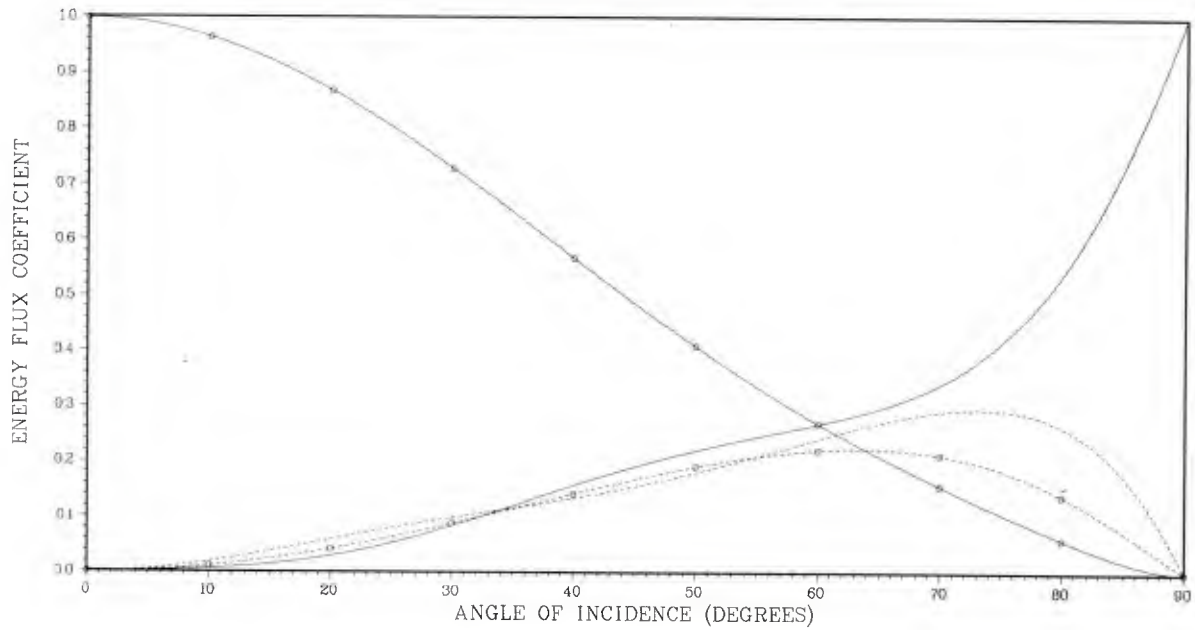


Figure 17a. Longitudinal Wave Incident on Aluminum/Lucite (.0355cm)/ Aluminum Structure at 7.5 MHz

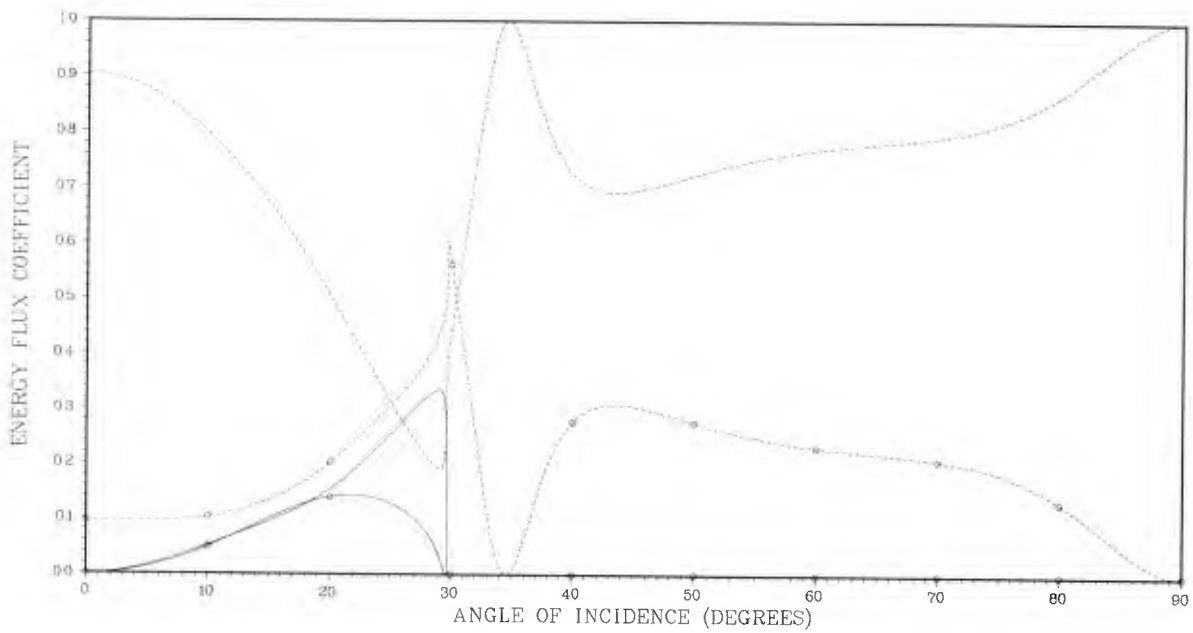


Figure 17b. Shear Wave Incident on Aluminum/Lucite (.019cm)/Aluminum Structure at 7.5 MHz

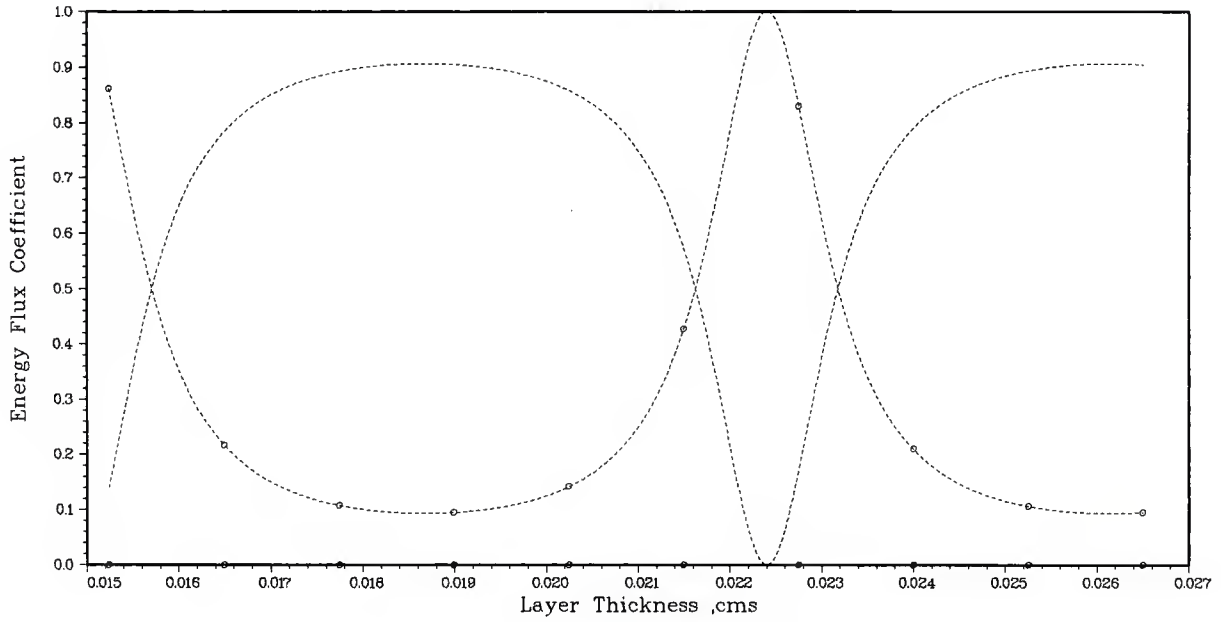


Figure 18a. Shear Wave Incident on Aluminum/Lucite/Aluminum Structure at 0° and 7.5 MHz

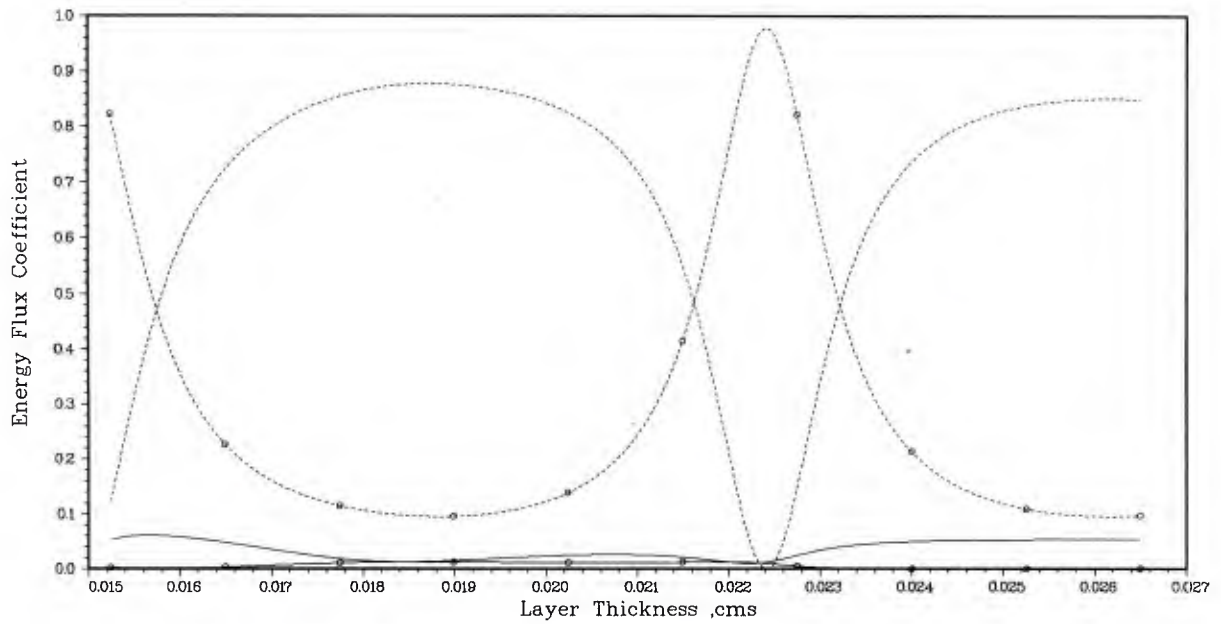


Figure 18b. Shear Wave Incident on Aluminum/Lucite/Aluminum Structure at 5° and 7.5 MHz

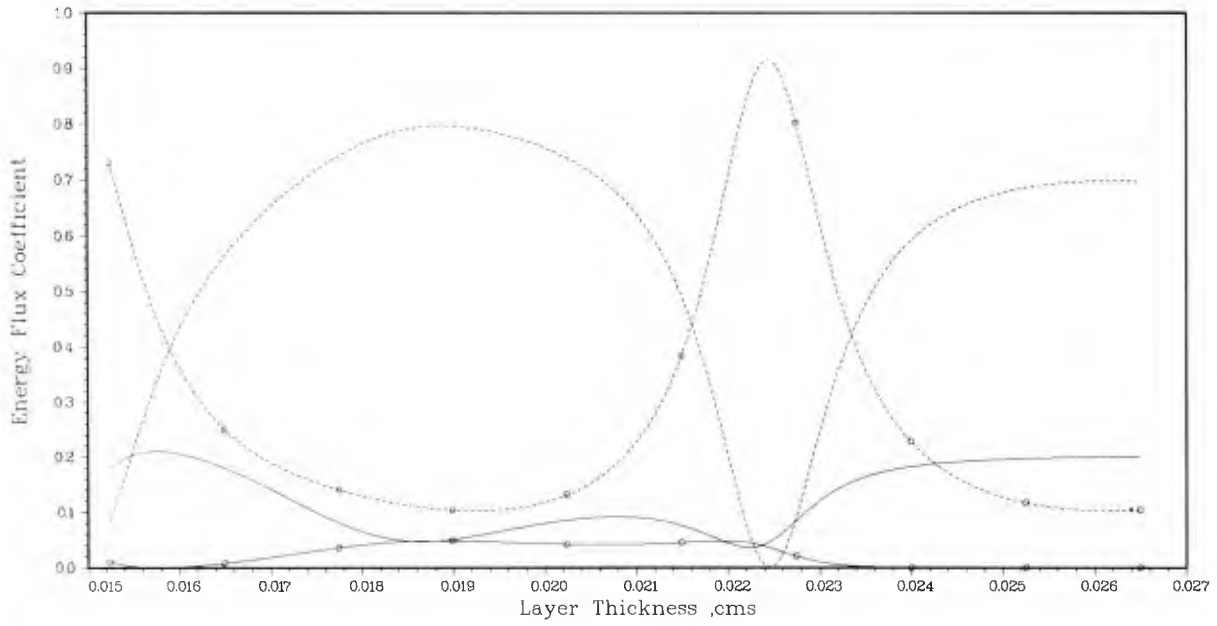


Figure 19a. Shear Wave Incident on Aluminum/Lucite/Aluminum Structure at 10° and 7.5 MHz

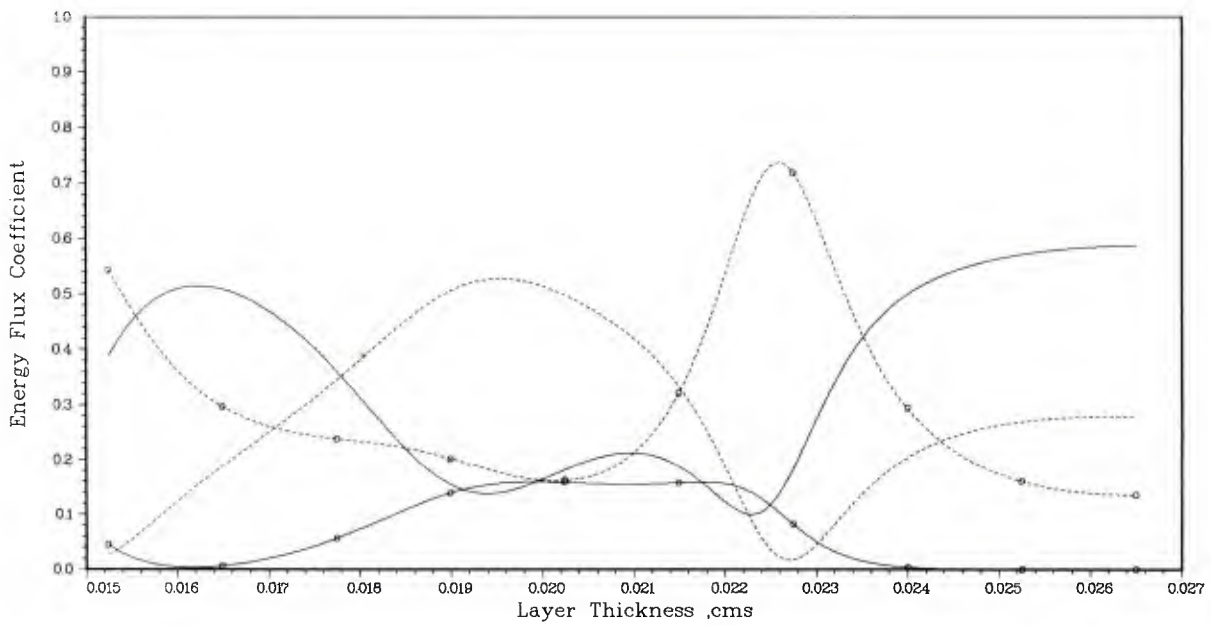


Figure 19b. Shear Wave Incident on Aluminum/Lucite/Aluminum Structure at 20° and 7.5 MHz

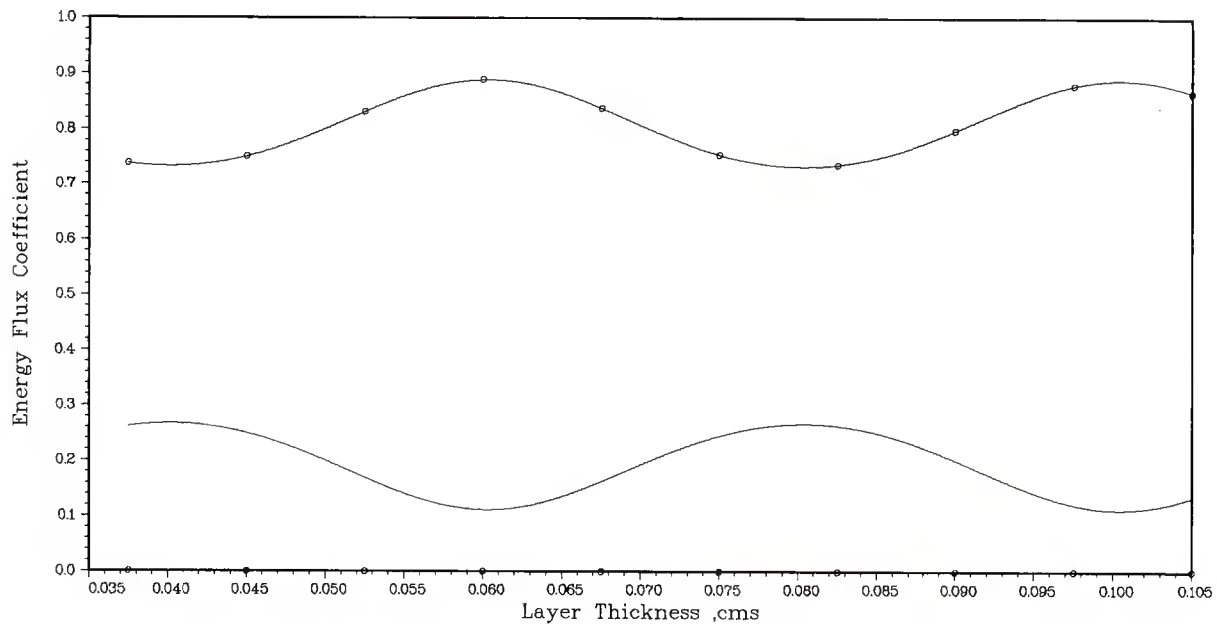


Figure 20a. Longitudinal Wave Incident on FE/VA/Quartz Structure at 0° and 7.5 MHz

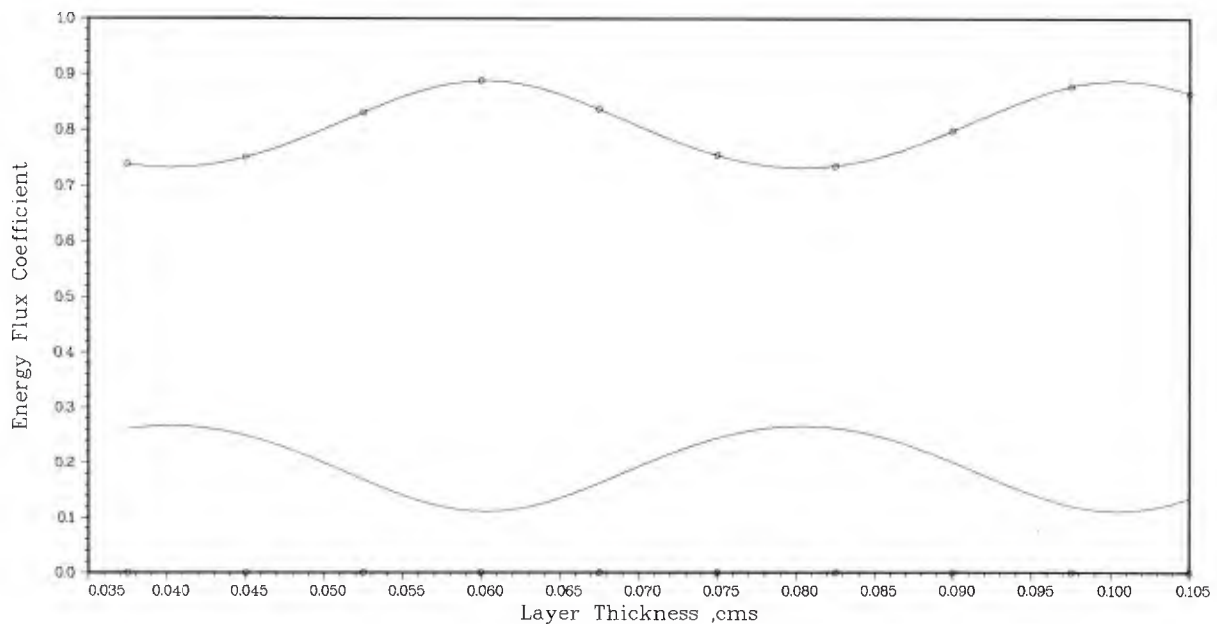


Figure 20b. Longitudinal Wave Incident on FE/VA/Quartz Structure at 5° and 7.5 MHz

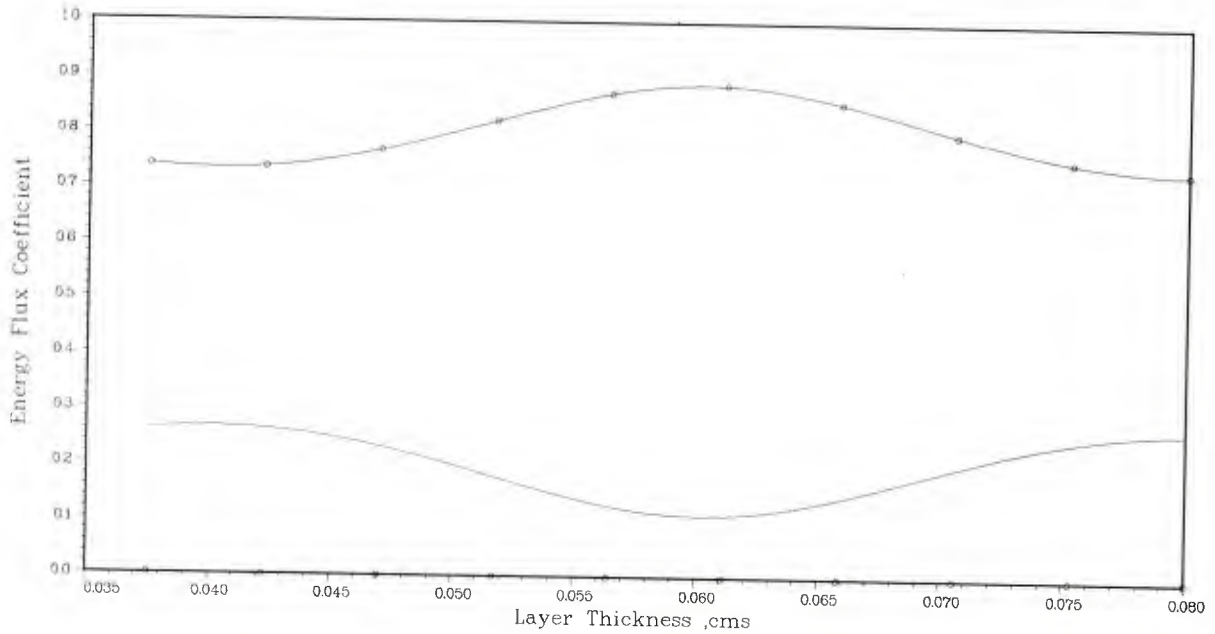


Figure 21a. Shear Wave Incident on FE/VA/Quartz Structure at 0° and 7.5 MHz

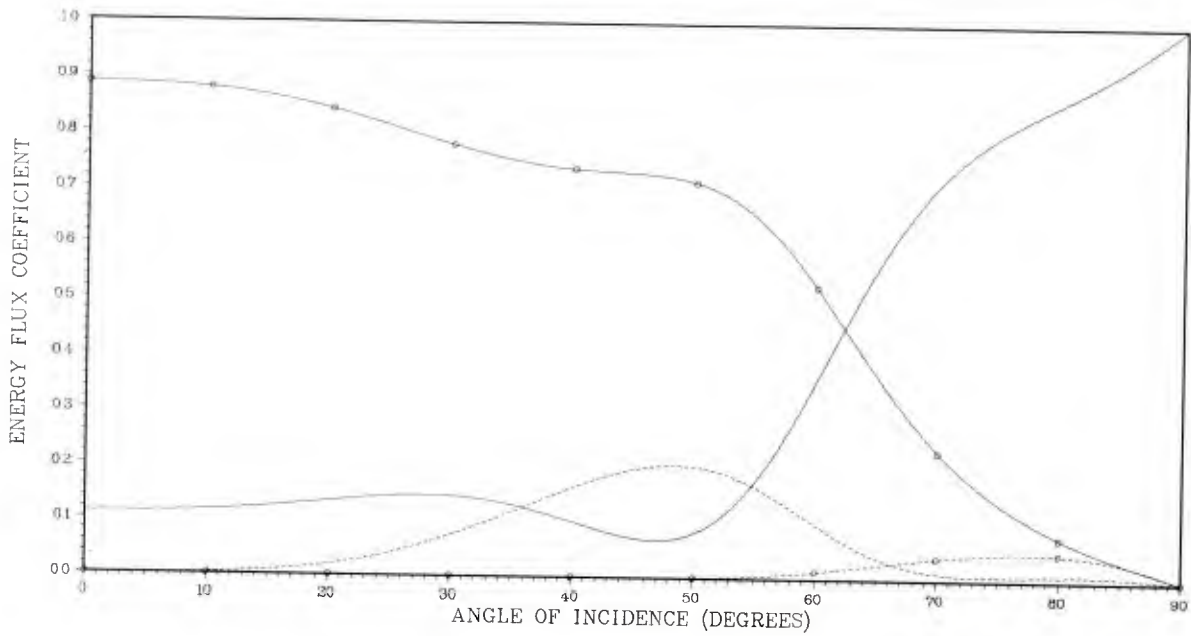


Figure 21b. Shear Wave Incident on FE/VA (.06cm)/Quartz Structure at 7.5 MHz

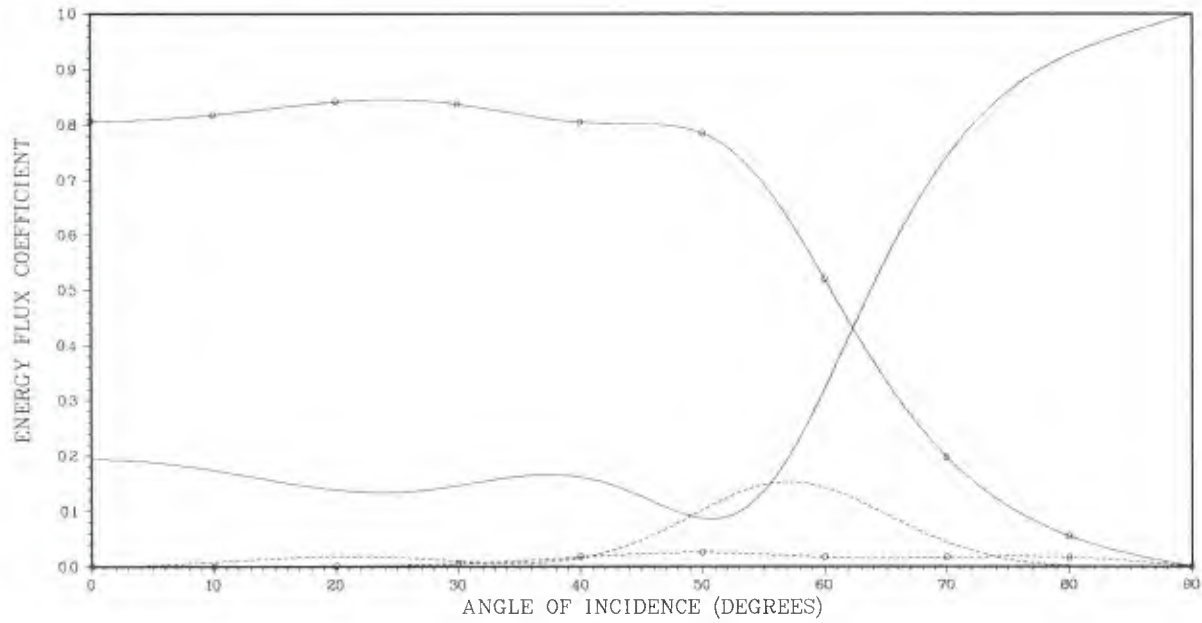


Figure 22. Shear Wave Incident on FE/VA (.07cm)/Quartz Structure at 7.5 MHz

SECTION IV

ACOUSTIC VELOCITY DATA

The following data on acoustic velocities in various materials have been collected from several reference tables as well as individual sources and are presented here as a convenience to the reader. Where practical, we have cited the original references rather than the compilations from which the data were actually taken. This procedure permits a more rapid access to the experimental literature, eliminating the necessity of searching through a second table to obtain additional information on a particular measurement. Although we have taken care to draw our data from sources we consider good and reliable and have double checked some entries against independent measurements, we must disclaim responsibility for their correctness.

LIQUIDS

Material	Temp. °C	Long.	Wavespeed	Surf.	Density gm/cm ³	Ref.
			Trans. 10 ⁵ cm/sec			
Acetic Acid	20	1.173			1.049	19
Acetic Anhydride	24	1.384			1.087	19
Acetone	20	1.192			0.792	19
Acetylacetone	20	1.416			0.970	19
Acetophenone	20	1.496			1.026	19
Acetylacetone	20	1.383			0.976	19
Acetylchloride	20	0.060			1.105	19
Acetylene Dichloride	25	1.025			1.265	19
Acetylene Tetra- bromide	20	1.041			2.963	19
Acetylene Tetra- chloride	28	1.155			1.578	19
Acrolein	20	1.207			0.841	19
iso-Amyl Alcohol	20	1.252				36
tert-Amyl Alcohol (dimethylethyl- carbinol)	28	1.204			0.809	19
Amyl Acetate	26	1.168			0.879	19
n-Amyl Bromide	20	0.981			1.246	19
Amyl Ether	26	1.153			0.774	19
iso-Amyl Ether	26	1.153				36
Amyl Formate	26	1.201			0.893	19
Aniline	20	0.656			1.022	19
Biacetyl	25	1.236			0.990	19
Benzaldehyde	20	1.479			1.050	19
Benzene	20	1.326			0.879	19

LIQUIDS

Material	Temp. °C	Long.	Wavespeed	Surf.	Density gm/cm ³	Ref.
			Trans. 10 ⁵ cm/sec			
Benzol	20	1.33			0.878	23
Bensophenone	100	1.316			1.107	36
Benzylacetone	20	1.514			0.989	19
Benzyl Alcohol	20	1.540			1.050	19
Benzyl Chloride	20	1.420			1.1026	19
Bismuth (Molten)	271	1.635			10.07	19
Blood (Horse)	37	1.571				36
Bromal	20	0.966			2.30	19
Bromobenzene	50	1.074				36
Bromoform	20	0.928			2.890	19
1-Bromonaphthalene	20	1.372			1.487	19
2-Butanone (Ethyl Methyl Ketone)	20	1.207			0.805	19
n-Butyl Alcohol	20	1.268			0.810	19
sec-Butyl Alcohol	20	1.222			0.808	19
tert-Butyl Alcohol	20	1.155			0.789	19
n-Butyl Bromide	20	0.990			1.299	19
iso-Butyl Bromide	-104	1.450				36
n-Butyl Chloride	20	1.133			0.884	19
Butyl Formate (Butyl Methanoate)	24	1.199			0.911	19
n-Butyl Iodide	20	0.977			1.617	19
Butyric Acid	10	1.203			0.959	19
Cadmium (Molten)	321	2.222			8.02	19
Caprylic Acid	20	1.331			0.910	19

LIQUIDS

Material	Temp. °C	Long.	Wavespeed		Surf.	Density gm/cm ³	Ref.
			Trans.	10 ⁵ cm/sec			
Carbon Disulfide	20	1.158				1.263	29
Carbon Tetrachloride	20	0.938				1.595	19
Carvacrol	20	1.475				0.976	19
Cesium (Molten)	28.5	0.967				1.84	19
m-Chloronitrobenzene	40	1.386					36
Chlorobenzene	20	1.291				1.107	19
Chloroform	20	1.005				1.498	19
l-Chlorohexane	20	1.221				0.872	19
l-Chloronaphthalene	20	1.481				1.194	19
o-Chlorotoluene	20	1.344				1.0817	19
m-Chlorotoluene	20	1.326				1.072	19
p-Chlorotoluene	20	1.316				1.0697	19
Cinnamaldehyde	25	1.554				1.112	19
Citral b	20	1.442				0.888	19
o-Cresol	25	1.506				1.046	19
Crotonaldehyde	20	1.344				0.858	19
Cumene	20	1.342				0.862	19
Cyclohexane	20	1.284				0.779	19
Cyclohexanol	20	1.493				0.945	19
Cyclohexanone	20	1.449				0.948	19
Cyclohexene	20	1.305				0.811	19
Cyclohexylamine	20	1.435				0.819	19
Cyclohexyl Chloride	20	1.319				1.016	19
1,3-Cyclopentadiene	20	1.421				0.805	19

LIQUIDS

Material	Temp. °C	Long.	Wavespeed	Surf.	Density gm/cm ³	Ref.
			Trans. 10 ⁵ cm/sec			
Cyclopentanone	24	1.474			0.948	19
p-Cymene (p-isopropyltoluene)	28	1.308			0.857	19
1-Decene	20	1.250			0.741	19
n-Decyl Alcohol	20	1.402			0.829	19
2-Dibromoethylene	20	0.957			2.271	19
m-Dichlorobenzene	28	1.232			1.285	19
o-Dichlorobenzene	20	1.295			1.305	19
1,1-Dichloroethane	20	1.034			1.174	19
Diethyl Aldehyde	24	1.378			0.825	19
N,N-diethyl Aniline	20	1.482			0.935	19
Diethyl Ether	25	0.985			0.714	36
Diethylene Glycol	25	1.586			1.132	19
Diethylene Glycol Monoethyl Ether	30	1.296				36
Diethyl Ester Malonic Acid	22	1.386			1.055	19
2,3-Dimethylbutanoic Acid	20	1.280			0.928	19
Dimethyl Polysiloxane	20	0.912				
Di-n-propyl Ether	20	1.112			0.736	19
Diphenylether	24	1.469			1.0728	19
Diphenylmethane	28	1.501			1.001	19
n-Dodecyl Alcohol	30	1.388			0.831	19
Ethanol Amide	25	1.724				36
Ethyl Acetate	20	1.176			0.901	19

LIQUIDS

Material	Temp. °C	Long.	Wavespeed	Surf.	Density gm/cm ³	Ref.
			Trans. 10 ⁵ cm/sec			
Ethyl-aceto-acetate	23.5	1.417			1.025	19
Ethyl Acetylmalonate	22.5	1.348			1.085	19
Ethyl Adipate	22	1.376			1.009	19
Ethyl Alcohol	20	1.180			0.789	19
Ethyl Benzol	20	1.34			0.868	
Ethyl Bromide	28	0.892			1.428	19
Ethyl Butyrate	23.5	1.117			0.879	19
Ethyl Caprylate	28	1.263			0.867	19
Ethyl Carbonate	28	1.173			0.975	19
Ethyl Chloroethanoate	25.5	1.234			1.159	19
Ethylene Bromide	20	1.009			2.170	19
Ethylene Chloride	23	1.240			1.257	19
Ethylene Dibromide	24	1.014			2.179	36
Ethylene Dichloride	23	1.240			1.235	36
Ethylene Glycol	20	1.616			1.115	19
Ethylene Glycol Monomethyl Ether	30	1.339				36
Ethyl Ester Propionic Acid	23.5	1.185			0.8846	19
Ethyl Ether	20	1.008			0.714	19
Ethyl Formate	24	1.721			0.924	19
Ethyl Iodide	20	0.869			1.940	19
Ethyl-o-tolyl Ether	25	1.315			0.959	19
Ethyl Oxalate	22	1.392			1.084	19

LIQUIDS

Material	Temp. °C	Long.	Wavespeed Trans. 10 ⁵ cm/sec	Surf.	Density gm/cm ³	Ref.
Ethyl Phenyl Ketone (Propiophenone)	20	1.498			1.012	19
Ethyl p-Phthalate	23	1.471			1.123	19
Ethyl Succinate	22	1.378			1.040	19
Eugenol	30	1.482			1.065	36
Formaldehyde	25	1.587			0.815	36
Formamide	20	1.550			1.134	19
Formic Acid	20	1.287			1.226	19
Furfuryl Alcohol	25	1.450			1.1296	19
Gallium (Molten)	29.5	2.740			6.1	19
Gasoline	34	1.25			0.803	
Geranyl Acetate	28	1.328			0.917	19
Glycerin	20	1.923			1.261	19
Heptane	20	1.160			0.684	36
ℓ-Heptane	20	1,128			1.684	36
n-Heptane	20	1,162			0.684	19
Heptanoic Acid	20	1,312			0.913	19
1-Heptene	20	1.128			0.697	19
n-Heptyl Alcohol	20	1.341			0.823	19
Heptyne	30	1.159			0.733	36
Hexane	20	1.083			0.660	19
n-Hexane	30	1.060			0.649	36
n-Hexyl Alcohol	20	1.322			0.820	19
Hexylmethyl Ketone	24	1.324			0.818	19
Indan (Hydrindene)	20	1.403			0.965	19

LIQUIDS

Material	Temp. °C	Long.	Wavespeed	Surf.	Density gm/cm ³	Ref.
			Trans. 10 ⁵ cm/sec			
Indene	20	1.475			1.006	19
Indium (Molten)	156	2.215			7.06	19
Iodobenzene	30	1.113			1.832	19
1-Iodohexane	20	1.081			1.441	19
α-Ionon	20	1.432			0.930	19
Kerosene	25	1.315			0.82	36
Lead (Molten)	327	1.790			10.68	19
d-Linalool	20	1.341			0.863	19
Menthol	50	1.271			0.904	36
Mercury	20	1.451			13.546	19
	50	1.440				19
Mesityl Oxide	20	1.310			0.854	19
3-Methoxytoluene	26	1.385			0.976	19
Methyl Acetate	25	1.154			0.928	19
Methyl Alcohol	20	1.123			0.796	19
N-Methyl Aniline	20	1.586			0.986	19
Methyl Bromide	2	0.905			1.676	36
Methyl Chloro- ethanoate	26	1.331			1.227	19
Methyl Cyanide	20	1.304			0.783	19
Methylcyclohexane	20	1.247			0.7864	19
2-Methylcyclohexanol	25.5	1.421			0.937	19
3-Methyl-1-cyclo- hexanol	25.5	1.406			0.914	19

LIQUIDS

Material	Temp. °C	Long.	Wavespeed	Surf.	Density gm/cm ³	Ref.
			Trans. 10 ⁵ cm/sec			
4-Methylcyclohexanol	25.5	1.387			0.913	19
2-Methylcyclohexanone	25.5	1.353			0.924	19
4-Methylcyclohexanone	25.5	1.348			0.913	19
Methylene Bromide	24	0.971			2.4953	19
Methylene Chloride	20	1.092			1.336	19
Methylene Iodide	24	0.977			3.325	19
Methyl Ester Salicylic Acid	28	1.408			1.184	19
Methyl Iodide	20	0.834			2.279	19
Methyl Phenol Ether (Anisole)	26	1.353			0.9988	19
Methyl Propionate	24.5	1.215			0.915	19
Methyl Propyl Ketone (Diethyl Ketone)	24	1.314			0.816	19
Milk (Evaporated)	20	1.558			1.04	36
Monoethyl Ether	25	1.458			0.990	19
Morpholine	25	1.442			1.000	19
Nicotine	20	1.491			1.009	19
Nitrobenzene	20	1.473			1.199	19
2-Nitroethanol	20	1.578			1.270	19
Nitromethane	20	1.346			1.130	19
o-Nitrotoluene	20	1.432			1.163	19
m-Nitrotoluene	20	1.489			1.164	19
Nonane	20	1.248			0.718	19
1-Nonene	20	1.218			0.729	19
n-Nonyl Alcohol	20	1.391			0.828	19

LIQUIDS

Material	Temp. °C	Long.	Wavespeed Trans. 10 ⁵ cm/sec	Surf.	Density gm/cm ³	Ref.
n-Octane	20	1.197			0.703	19
1-Octanol	20	1.358			0.825	19
n-Octyl Bromide	20	1.182			1.116	19
n-Octyl Chloride	20	1.280			0.875	19
Oil						
Campor	25	1.390				36
Castor	19	1.500			0.969	36
Condenser	20	1.432				36
Olive	22	1.440			0.918	36
Petroleum	34	1.29			0.825	23
SAE 20	20	1.74			0.87	24
Sperm	32	1.411				36
Transformer	20	1.38			0.92	22
Oleic Acid	45	1.333			0.873	19
Paraldehyde	20	1.204			0.994	19
Pentachloroethane	20	1.113			1.709	19
1-Pentadecene	20	1.351			0.776	36
Pentane	20	1.008			0.626	19
n-Pentane	20	1.044				36
1-Pentanol	20	1.294			0.815	19
iso-Pentanol	21	1.255				36
Perchloroethylene	20	1.066			1.623	19
Phenetole	26	1.153			0.967	19

LIQUIDS

Material	Temp. °C	Long.	Wavespeed		Density gm/cm ³	Ref.
			Trans.	Surf.		
			10 ⁵ cm/sec			
Phenol	100	1.274			1.072	36
Phenylethane	20	1.338			0.867	19
Phenylhydrazine	20	1.738			1.098	19
Phenyl Mustard Oil	27	1.412			1.131	19
α-Picoline	28	1.453			0.951	19
β-Picoline	28	1.419			0.961	19
dl-Pinene	24	1.247			0.858	19
Piperidine	20	1.400			0.862	19
Polymethyl Siloxane	20	1.019				36
Potassium (Molten)	64	1.820			0.82	19
Propionic Acid	20	1.176			0.992	19
n-Propionitrile	20	1.271			0.783	19
n-Propyl Acetate	26	1.182			0.887	19
n-Propyl Alcohol	20	1.223			0.804	19
n-Propyl Chloride	20	1.091			0.890	19
n-Propyl Iodide	20	0.929			1.747	19
Pseudocumene	20	1.368			0.876	19
Pyridine	20	1.445			0.982	19
Quinaldine	20	1.575			1.1013	19
Quinaline	20	1.600			1.095	19
Resorcinol Dimethyl Ether	26	1.460			1.080	19
Rubidium (Molten)	39	1.260			1.46	19
Salicylaldehyde	27	1.474			1.166	19

LIQUIDS

Material	Temp. °C	Long.	Wavespeed		Surf.	Density gm/cm ³	Ref.
			Trans.	10 ⁵ cm/sec			
Silicon Tetrachloride	30	0.766				1.483	36
Sodium (Molten)	98	2.395				0.93	19
Sodium Carbonate	903	2.300					19
Sodium Chloride	864	1.726					19
Sodium Sulfide	960	2.037					19
Tetrachloroethylene	28	1.027				1.623	19
Tetraethylethylene Glycol	25	1.586				1.123	19
Tetranitromethane	20	1.039				1.650	19
Thiolacetic Acid	20	1.168				1.074	19
Thiophene	20	1.300				1.065	19
Toluene	20	1.328				0.867	19
o-Toluidene	20	1.634				1.004	19
m-Toluidene	20	1.620				1.989	19
1,2,4-Trichlorobenzene	20	1.301				1.456	19
Trichloroethylene	20	1.049				1.477	19
Tridecylene	20	1.313				0.798	19
Triethylene Glycol	25	1.608				1.125	19
Trimethylene Bromide	23.5	1.144				1.979	19
Triolein	20	1.482				0.915	19
Water (Distilled)	20	1.482				1.00	36
Water (Heavy, D ₂ O)	19.8	1.383				1.11	36
o-Xylene	20	1.360				0.880	19
m-Xylene	20	1.340				0.864	19
p-Xylene	20	1.330				0.861	19

SOLIDS - METALS

Material	Temp. °C	Long.	Wavespeed		Surf.	Density gm/cm ³	Ref.
			Trans.	10 ⁵ cm/sec			
Aluminum	20	6.374	3.111		2.906	2.70	24
Al 1100	20	6.31	3.08			2.71	25
Al 2014	20	6.37	3.07			2.80	34
Al 2024-T4	20	6.37	3.16		2.95	2.77	35
Al 2117-T4	20	6.50	3.12			2.80	27
Al 6061-T6	20	6.31	3.14			2.70	50
Bearing Babbit	20	2.30				10.1	35
Beryllium	20	12.890	8.880		7.87	1.82	19
Bismuth	20	2.18	1.10			9.80	19
Brass (Alpha)	20	4.28	2.02			8.45	28
Brass (70% Cu - 30% Zn)	20	4.37	2.10			8.50	19
Brass (Naval)	20	4.43	2.12			8.42	19
Bronze (Phosphor 5%)	20	3.53	2.23			8.86	19
Cadmium	20	2.780	1.50			8.64	19
Cerium	20	2.424	1.415			6.77	43
Chromium	20	6.608	4.005			7.2	36
Cobalt	20	5.88	3.10			8.9	39
Columbium	20	4.92	2.10			8.57	28
Columbium (10W,10TA)	20	5.13	1.90				35
Constantan	20	5.177	2.625		2.445	8.88	36
Copper	20	4.759	2.325		2.171	8.93	36
Copper 110	20	4.70	2.26			8.9	37

SOLIDS - METALS

Material	Temp. °C	Long.	Wavespeed		Surf.	Density gm/cm ³	Ref.
			Trans.	10 ⁵ cm/sec			
Dysprosium	20	2.926	1.733			8.53	42
Erbium	20	2.064	1.807			9.06	42
Europium	20	1.931	1.237			5.17	44
Gadolinium	20	2.927	1.677			7.89	42
Germanium	20	5.18	3.10			5.47	39
Gold	20	3.24	1.20			19.32	19
Hafnium	20	2.84				13.3	35
Hastelloy X	20	5.79	2.74			8.23	19
Hastelloy C	20	5.84	2.90			8.94	19
Holmium	20	3.089	1.729			8.80	42
Indium	20	2.56	0.74			7.30	39
Invar (36 Ni, 63.8 Fe, 0.2 C)	20	4.657	2.658	2.447			36
Lanthanum	20	2.362	1.486			6.16	41
Lead							
Pure	20	2.160	0.700	0.64		11.34	19
Hard (94Pb-6Sb)	20	2.16	0.81			10.88	19
Lutetium	20	2.765	1.574			9.85	41
Magnesium	20	5.823	3.163	2.930		1.74	36

SOLIDS - METALS

Material	Temp. °C	Wavespeed			Density gm/cm ³	Ref.
		Long.	Trans.	Surf.		
		10 ⁵ cm/sec				
Magnesium AM-35	20	5.79	3.10	2.87	1.74	19
Magnesium FS-1	20	5.47	3.03		1.69	26
Magnesium J-1	20	5.67	3.01		1.70	26
Magnesium M1A	20	5.74	3.10	2.87	1.76	37
Magnesium O-1	20	5.80	3.04		1.82	26
Manganese	20	4.66	2.35		7.39	24
Manganin	20	4.66	2.35		8.40	19
Molybdenum	20	6.29	3.35	3.11	10.2	19
Nickel						
Pure	20	5.63	2.96		8.88	20
Inconel	20	5.82	3.02	2.79	8.5	35
Inconel (X-750)	20	5.94	3.12		8.3	19
Inconel (Wrought)	20	7.82	3.02		8.25	19
Monel	20	5.35	2.72		8.83	36
Monel (Wrought)	20	6.02	2.72		8.83	20
Silver-Nickel (18%)	20	4.62	2.32		8.75	19
German-Silver	20	4.76	2.16		8.40	16
Neodymium	20	2.751	1.502		7.01	45
Platinum	20	3.96	1.67		21.4	19
Potassium	20	2.47	1.22		0.862	39
Praseodymium	20	2.639	1.437		6.75	45
Samarium	20	2.875	1.618		7.48	45
Silver	20	3.60	1.59		10.5	19

SOLIDS - METALS

Material	Temp. °C	Long.	Wavespeed		Surf.	Density gm/cm ³	Ref.
			Trans.	10 ⁵ cm/sec			
Sodium	20	3.03	1.70			0.97	39
Steel							
1020	20	5.89	3.24			7.71	35
1095	20	5.90	3.19			7.80	35
4150, Rc14	20	5.86	2.79			7.84	35
4150, Rc18	20	5.88	3.18			7.82	30
4150, Rc43	20	5.87	3.20			7.81	30
4150,Rc64	20	5.83	2.77			7.80	30
4340	20	5.85	3.24			7.80	31
Carbon Steel (Annealed)	20	5.94	3.24		3.0	7.85	37
Iron (Cast)	20	3.5-5.6	2.2-3.2		2.5-3.0	6.95-7.35	37
52100 Steel							
Annealed	20	5.99	3.27			7.83	37
Hardened	20	5.89	3.20			7.8	37
D6 Tool Steel							
Annealed	20	6.14	3.31			7.7	37
Hardened	20	6.01	3.22			7.7	37
Stainless Steel							
Type 302	20	5.66	3.12			7.9	37
Type 304L	20	5.64	3.07			7.9	37
Type 347	20	5.74	3.10			7.91	37
Type 410	20	5.39	2.99			7.67	37
Type 430	20	6.01	3.36			7.7	37
Tantalum	20	4.10	2.90			16.6	35

SOLIDS - METALS

Material	Temp. °C	Wavespeed		Surf.	Density gm/cm ³	Ref.
		Long.	Trans.			
		10 ⁵ cm/sec				
Terbium	20	2.939	1.666		8.27	42
Thallium	302	1.62			11.9	23
Thorium	20	2.94	1.56		11.3	28
Thulium	20	3.009	1.809		9.29	46
Tin	20	3.32	1.67		7.29	19
Titanium	20	6.07	3.11		4.50	35
Titanium (6Al, 4V)	20	6.18	3.29		4.50	50
Tungsten						
Annealed	20	5.221	2.887	2.668	19.25	36
Drawn	20	5.410	2.640			36
Uranium	20	3.37	1.98		18.7	32
Vanadium	20	6.023	2.774	2.600	6.03	28
Ytterbium	20	1.946	1.193		6.99	46
Yttrium	20	4.10	2.38		4.34	39
Zinc	20	4.187	2.421	2.225	7.10	24
Zirconium	20	4.65	2.25		6.48	28

SOLIDS - CERAMICS

Material	Temp. °C	Long.	Wavespeed		Surf.	Density gm/cm ³	Ref.
			Trans.	10 ⁵ cm/sec			
Ammonium Dihydrogen Phosphate (ADP)							
X-Cut	20	6.250					36
Y-Cut	20	6.250					36
Z-Cut	20	4.300					36
Aluminum							
Oxide (Al ₃ O ₃)	20	10.84	6.36			3.98	49
Barium Nitrate	20	4.12	2.28			3.24	39
Barium Titanate	20	5.65	3.03			5.5	51
Bone (Human Tibia)	20	4.00	1.97			1.7-2.0	36
Cobalt Oxide (CoO)	23	6.56	3.32			6.39	48
Concrete	20	4.25 -5.25				2.60	36
Glass							
Crown	20	5.66	3.42			2.50	19
Flint	20	4.26	2.56			3.60	19
Lead	20	3.760	2.220			4.6	19
Plate	20	5.77	3.43			2.51	19
Pyrex	20	5.57	3.44			2.23	19
Quartz	20	5.57	3.51			2.60	19
Soft	20	5.40				2.40	19
Granite	20	3.95				2.75	19
Graphite	20	4.21	2.03			2.25	39
Ice	-16	3.83	1.92			0.94	51
Indium Antimonide	20	3.59	1.91				39
Lead Nitrate	20	3.28	1.47			4.53	39
Lithium Fluoride	20	6.56	3.84			2.64	39

SOLIDS - CERAMICS

Material	Temp. °C	Long.	Wavespeed	Surf.	Density gm/cm ³	Ref.
			Trans. 10 ⁵ cm/sec			
Magnesium Oxide (MgO)	20	9.32	5.76		3.58	39
Manganese Oxide (MnO)	23	6.68	3.59		5.37	48
Nickel Oxide (NiO)	23	6.60	3.68		6.79	48
Porcelain	20	5.34	3.12		2.41	19
Quartz						
Natural	20	5.73			2.65	19
Fused	20	5.57	3.52		2.60	19
Polycrystalline	20	5.75	3.72		2.65	51
Rock Salt	20	4.60	2.71		2.17	39
Rutile (TiO ₂)	20	8.72	4.44		4.26	39
Sandstone	20	2.920	1.840		2.2-2.4	36
Sapphire (c-axis)	20	11.91	7.66		3.97	55
Silicon	20	8.81	5.17			39
Slate	20	4.50			2.6-3.3	
Sulphur	115	1.35			1.803	
Titanium Carbide	20	8.27	5.16		5.15	20
Tourmaline (Z-Cut)	20	7.54			3.10	36
Tungsten Carbide	20	6.66	3.98		10-15	19
Yttrium Iron Garnet	20	7.29	4.41		5.17	39
Zinc Sulfide	20	5.17	2.42		4.02	39
Zinc Oxide	20	6.00	2.84		5.61	39

SOLIDS - POLYMERS

Material	Temp. °C	Long.	Wavespeed		Surf.	Density gm/cm ³	Ref.
			Trans.	10 ⁵ cm/sec			
Acrylic Resin	20	2.67	1.12			1.18	20
Bakelite	20	2.59				1.40	22
Bakelite (Cloth Filled)	20	2.71					35
Butyl Rubber	20	1.990				1.13	38
Butyl Rubber/Carbon (100/40)	20	1.600					36
Cellulose Acetate	20	2.45				1.30	33
Cork	20	0.5				0.2	19
Delrin (Acetalhomo-polymer)	0	2.515				1.42	47
Ebonite	20	2.500				1.15	36
Kel-F	20	1.79					35
Lexan (Polycarbonate)	0	2.280				1.19	47
Micarta (Linen Base)	20	3.00					35
Neoprene	20	1.730				1.42	38
Neoprene/Carbon (100/60)	20	1.690					36
Nylon	20	2.680					36
Nylon 6,6	20	1.68					23
Paraffin	20	2.20				0.83	37
Perspex	20	2.70	1.33		1.24	1.29	36
Phenolic	20	1.42				1.34	35
Plexiglas							
UVA	20	2.76				1.27	24
UVA II	20	2.73	1.43			1.18	24

SOLIDS - POLYMERS

Material	Temp. °C	Long.	Wavespeed	Surf.	Density gm/cm ³	Ref.
			Trans. 10 ⁵ cm/sec			
Polyacrylonitrile- butadiene-styrene I	20	2.160	0.930		1.041	38
Polyacrylonitrile- butadiene-styrene II	20	2.020	0.810		1.022	38
Polybutadiene Rubber	20	1.570			1.10	38
Polycaprolactam	20	2.700	1.120		1.146	38
Polycarboranesiloxane	20	1.450			1.041	38
Polydimethylsiloxane	20	1.020			1.045	38
Polyepoxide + glass spheres I	20	2.220	1.170		0.691	38
Polyepoxide + glass spheres II	20	2.400	1.280		0.718	38
Polyepoxide + glass spheres III	20	2.100	1.020		0.793	38
Polyepoxide + MPDA	20	2.820	1.230		1.205	38
Polyester + water	20	1.840	0.650		1.042	38
Polyethylene	20	2.67			1.10	22
Polyethylene TCI (mol. wt. 19000)	20	1.60				23
Polyethylene Oxide	20	1.60				23
Polyhexamethylene adipamide	20	2.710	1.120		1.147	38
Polymethylmethacrylate	20	2.690	1.344		1.191	38
Polyoxmethylen	20	2.440	1.000		1.425	38
Polypropylene	20	2.650	1.300		0.913	38
Polystyrene	20	2.400	1.150		1.052	22
Polystyrol (mol. wt. 40000)	20	1.50				23
Polysulfane Resin	20	2.297			1.24	47

SOLIDS - POLYMERS

Materials	Temp. °C	Long.	Wavespeed	Surf.	Density gm/cm ³	Ref.
			Trans. 10 ⁵ cm/sec			
Polytetrafluoro- ethylene (Teflon)	20	1.380			2.177	38
Polyvinylbutyral	20	2.350			1.107	38
Polyvinyl chloride	20	2.300				36
Polyvinyl chloride acetate	20	2.250				36
Polyvinyl formal	20	2.680				36
Polyvinylidene chloride	20	2.400				36
Polyvinylidene fluoride	20	1.930			1.779	38
Rubber						
India	20	1.48			0.90	19
Natural	20	1.550			1.12	38
Rubber/Carbon (100/40)	20	1.680				35
Silicon Rubber	20	0.948			1.48	47

APPENDIX

We present in this appendix the elements of the transformation matrix $\{T;n\}$ from Equation 17. The following definitions are made for convenience:

$$A = \alpha d, \quad B = \beta d, \quad \sigma = \beta/q. \quad (A1)$$

Since it is understood that all quantities, except the frequency ω and the x-projection of the wavevector q , are functions of the layer index n , we have dropped the superscript notation for simplicity:

$$T_{11} = (2\cos A + (\sigma^2 - 1)\cos B)/(\sigma^2 + 1) \quad (A2)$$

$$T_{12} = i[(\sigma^2 - 1)(q/\alpha)\sin A - 2\sigma\sin B]/(\sigma^2 + 1) \quad (A3)$$

$$T_{13} = (q/\rho\omega)[\cos B - \cos A] \quad (A4)$$

$$T_{14} = -i[(q^2/\rho\omega\alpha)\sin A + (\beta/\rho\omega)\sin B] \quad (A5)$$

$$T_{21} = i[(2\alpha/q)\sin A - (\sigma - \alpha^{-1})\sin B] \quad (A6)$$

$$T_{22} = [(\sigma^2 - 1)\cos A + 2\cos B]/(\sigma^2 + 1) \quad (A7)$$

$$T_{23} = -i[(\alpha/\rho\omega)\sin A + (q^2/\rho\omega\beta)\sin B] \quad (A8)$$

$$T_{24} = T_{13} \quad (A9)$$

$$T_{31} = 2\rho\omega(1 - \sigma^2)(\cos A - \cos B)/q(\sigma^2 + 1)^2 \quad (A10)$$

$$T_{32} = -i[(\rho\omega/\alpha)(\sigma^2 - 1)^2\sin A + 4(\rho\omega\sigma/q)\sin B]/(\sigma^2 + 1)^2 \quad (A11)$$

$$T_{33} = T_{22} \quad (A12)$$

$$T_{34} = T_{12} \quad (A13)$$

$$T_{41} = -i[4(\rho\omega\alpha/q^2)\sin A + (\rho\omega/\beta)(\sigma^2 - 1)^2\sin B](\sigma^2 + 1)^2 \quad (\text{A14})$$

$$T_{42} = T_{31} \quad (\text{A15})$$

$$T_{43} = T_{21} \quad (\text{A16})$$

$$T_{44} = T_{11} \quad (\text{A17})$$

An interesting property of $\{T;n\}$ is that for $d = 0$, it reduces to the identity matrix. We may therefore treat the problem of reflection at a single interface as a degenerate three-medium problem, where the remaining properties of the second medium are irrelevant since its thickness is zero.

REFERENCES

1. J. W. S. Rayleigh, The Theory of Sound, 2nd ed., Dover Publications, New York (1945), Chap. 13.
2. W. T. Thomson, J. Appl. Phys. 21, 89 (1950); ibid. 21, 1215 (1950).
3. D. L. Folds and C. D. Loggins, J. Acoust. Soc. Am. 62, 1102 (1977).
4. N. Haskell, Bull. Seismol. Soc. Am. 43, 17 (1953).
5. R. B. Lindsay, J. Acoust. Soc. Am. 11, 178 (1939); J. B. Smyth and R. B. Lindsay, ibid. 16, 20 (1944).
6. L. M. Brekhovskish, Waves in Layered Media, Academic Press, New York (1960) Chap. 1.
7. J. P. Achenbach, Wave Propagation in Elastic Solids, North Holland, Amsterdam (1973).
8. W. M. Ewing, W. S. Jardetzky, and F. Press, Elastic Waves in Layered Media, McGraw-Hill, New York (1957).
9. R. N. Thurston, in Physical Acoustics, Vol. I-A, ed. by W. P. Mason, Academic Press, New York (1964) p.77.
10. W. P. Mason, Physical Acoustics and the Properties of Solids, Van Nostrand, Princeton (1958).
11. D. L. Arenberg, J. Acoust. Soc. Am. 20, 1 (1948).
12. G. Herrmann, R. K. Kaul, and T. J. Delph, Arch. Mech. 28, 405 (1976).
13. M. Comninou and J. Dundurs, Proc. R. Soc. Lond. A 356, 509 (1977).
14. R. M. Christensen, J. Appl. Mech. 42, 153 (1975).
15. Yu. K. Engel'brekht, Sov. Phys. Acoust. 23, 102 (1977).
16. W. R. Scott and P. F. Gordon, J. Acoust. Soc. Am. 62, 108 (1977).
17. A. P. Wills, Vector Analysis with an Introduction to Tensor Analysis, Dover Publications, New York (1958) p. 121.
18. J. D. Jackson, Classical Electrodynamics, 2nd ed., John Wiley & Sons, Inc., New York (1975), p. 279.
19. D. Ensminger, Ultrasonics, Marcel Dekker, New York (1973) pp. 198-219.
20. H. E. von Valkenburg, in Nondestructive Testing Handbook, ed. by R. C. Masters, The Ronald Press, New York (1959), Chap. 43.

REFERENCES (CONTINUED)

21. Handbook of Chemistry and Physics, ed. by R. C. Weast, The Chemical Rubber Co., Cleveland (1972).
22. B. Carlin, Ultrasonics, McGraw-Hill, New York (1960).
23. L. Bergmann, Der Ultraschall, Hirzel Verlag, Stuttgart (1954).
24. J. Krautkramer and H. Krautkramer, Werkstoffpruefung mit Ultraschall, Julius Springer-Verlag, Berlin (1961).
25. W. Roty, J. Appl. Physics 19, 901 (1948).
26. F. A. Metz and W. M. A. Andersen, Electronics 22, 96 (1949).
27. W. P. Mason and H. J. McSkimin, Bell Syst. Tech. J. 31, 122 (1952).
28. Data provided by Reynolds Aluminum Co.
29. H. J. McSkimin, J. Acoust. Soc. Am. 22, 413 (1950).
30. R. Roderick and R. Truell, Wright Aeronautical Laboratory Report No. 143/14-14.
31. Firestone Corp. Patent No. 2439130.
32. Data provided by Hanford Atomic Laboratory.
33. W. P. Mason, Piezoelectric Crystals and their Applications to Ultrasonics, Van Nostrand, New York (1950).
34. Sperry Corp. Document No. 50K-18.
35. Data provided by Automation Industries, Inc.
36. G. W. C. Kaye and T. H. Laby, Tables of Physical and Chemical Constants, 14th ed., Longman, London
37. H. E. Boyer, ed., Metals Handbook, Vol. II, 8th ed., American Society for Metals, Metals Park, Ohio (1976).
38. B. Hartmann and J. Jarzynski, J. Acoust. Soc. Am. 56, 1496 (1974).
39. E. Papadakis, J. Acoust. Soc. Am. 37, 703 (1965).
40. H. Wang, J. Geophys. Res. 80, 3761 (1975).
41. K. L. Navayang, Acoustica 39, 336 (1978).
42. M. Rosen, Phys. Rev. 174, 504 (1968).
43. M. Rosen, Phys. Rev. 181, 932 (1969).

REFERENCES (CONCLUDED)

44. M. Rosen, Phys. Rev. 166, 561 (1968).
45. M. Rosen, Phys. Rev. 180, 540 (1969).
46. M. Rosen, Phys. Chem. Solids 32, 2351 (1971).
47. D. L. Folds, J. Acoust. Soc. Am. 52, 426 (1972).
48. N. Uchida and S. Saito, J. Acoust. Soc. Am. 51, 1602 (1972).
49. R. Ruh, Private Communication.
50. M. P. Hagelberg, Private Communication.
51. R. Truell, C. Elbaum, and B. Chick, Ultrasonic Methods in Solid State Physics, Academic Press, New York (1969) p. 369.